

การเปรียบเทียบความแนบตามชอบกับเนื้อฟันและความพรุนของไบโอดีนทีนและเอ็มทีเอในการซ่อม
รอยทะลุง่ามรากฟันภายใต้สภาวะปนเปื้อนเลือด



นายรังสิต เมฆารักษ์ภิญโญ

จุฬาลงกรณ์มหาวิทยาลัย
CHULALONGKORN UNIVERSITY

บทคัดย่อและแฟ้มข้อมูลฉบับเต็มของวิทยานิพนธ์ตั้งแต่ปีการศึกษา 2554 ที่ให้บริการในคลังปัญญาจุฬาฯ (CUIR)
เป็นแฟ้มข้อมูลของนิสิตเจ้าของวิทยานิพนธ์ ที่ส่งผ่านทางบัณฑิตวิทยาลัย

The abstract and full text of theses from the academic year 2011 in Chulalongkorn University Intellectual Repository (CUIR)
are the thesis authors' files submitted through the University Graduate School.

วิทยานิพนธ์นี้เป็นส่วนหนึ่งของการศึกษาตามหลักสูตรปริญญาวิทยาศาสตรมหาบัณฑิต

สาขาวิชาวิทยาเอ็นไอโอดอนด์ ภาควิชาทันตกรรมหัตถการ

คณะทันตแพทยศาสตร์ จุฬาลงกรณ์มหาวิทยาลัย

ปีการศึกษา 2558

ลิขสิทธิ์ของจุฬาลงกรณ์มหาวิทยาลัย

COMPARISON OF MARGINAL ADAPTATION TO DENTINE AND POROSITY OF BIODENTINE
AND MTA IN BLOOD CONTAMINATED FURCATION REPAIR

Mr. Rangsit Makarukpinyo



A Thesis Submitted in Partial Fulfillment of the Requirements
for the Degree of Master of Science Program in Endodontology

Department of Operative Dentistry

Faculty of Dentistry

Chulalongkorn University

Academic Year 2015

Copyright of Chulalongkorn University

Thesis Title	COMPARISON OF MARGINAL ADAPTATION TO DENTINE AND POROSITY OF BIODENTINE AND MTA IN BLOOD CONTAMINATED FURCATION REPAIR
By	Mr. Rangsit Makarukpinyo
Field of Study	Endodontology
Thesis Advisor	Assistant Professor Chootima Ratisoontorn, Ph.D.

Accepted by the Faculty of Dentistry, Chulalongkorn University in Partial
Fulfillment of the Requirements for the Master's Degree

.....Dean of the Faculty of Dentistry
(Suchit Poolthong, Ph.D.)

THESIS COMMITTEE

.....Chairman
(Associate Professor Piyanee Panitvisai)

.....Thesis Advisor
(Assistant Professor Chootima Ratisoontorn, Ph.D.)

.....Examiner
(Assistant Professor Anchana Panichuttra, Ph.D.)

.....External Examiner
(Jaruma Sakdee, D.M.Sc)

รังสิต เมฆารักษ์ภิญโญ : การเปรียบเทียบความแนบตามขอบกับเนื้อฟันและความพรุนของไบโอเด็นทีนและเอ็มทีเอในการซ่อมรอยทะลุง่ามรากฟันภายใต้สภาวะปนเปื้อนเลือด (COMPARISON OF MARGINAL ADAPTATION TO DENTINE AND POROSITY OF BIODENTINE AND MTA IN BLOOD CONTAMINATED FURCATION REPAIR) อ.ที่ปรึกษาวิทยานิพนธ์หลัก: ผศ. ทญ. ดร. ชุตินา ระติสุนทร , 73 หน้า.

บทนำ: การศึกษานี้มีจุดประสงค์เพื่อเปรียบเทียบความพรุนและความแนบตามขอบกับเนื้อฟันของไบโอเด็นทีนและเอ็มทีเอในสภาวะที่มีและไม่มีกรปนเปื้อนเลือดในการซ่อมรอยทะลุง่ามรากฟันโดยใช้เครื่องมือคอมพิวเตอร์ทอมोगราฟฟี (Microcomputed Tomography (micro-CT)) วิธีวิจัย: รอยทะลุง่ามรากฟันถูกเตรียมบนฟันกรามล่างซี่ที่ 1 ของมนุษย์ที่ถูกถอนออกมาจำนวน 64 ซี่ แบ่งตัวอย่างออกเป็น 4 กลุ่ม คือ กลุ่มไบโอเด็นทีนที่ปนเปื้อนเลือด (Biodentine/Blood) กลุ่มไบโอเด็นทีนที่ปนเปื้อนน้ำเกลือ (Biodentine/NSS) กลุ่มเอ็มทีเอที่ปนเปื้อนเลือด (MTA/Blood) และกลุ่มเอ็มทีเอที่ปนเปื้อนน้ำเกลือ (MTA/NSS) ทำการกราดตรวจตัวอย่างทุกชิ้นโดยเครื่อง Micro-CT ที่เวลาซึ่งตัวเริ่มแรกของวัสดุแต่ละชนิดและที่เวลา 24 ชั่วโมง ค่าเฉลี่ยร้อยละของปริมาตรของช่องว่างระหว่างวัสดุและเนื้อฟันได้จากการคำนวณความแตกต่างของปริมาตรรอยทะลุง่ามรากฟันกับปริมาตรของวัสดุ ค่าเฉลี่ยร้อยละของความพรุนได้โดยตรงจากรายงานของเครื่อง Micro-CT ผลการวิจัย: การปนเปื้อนเลือดเพิ่มค่าเฉลี่ยร้อยละของปริมาตรของช่องว่างระหว่างวัสดุและเนื้อฟันอย่างมีนัยสำคัญทางสถิติในวัสดุทั้งสองชนิด ($P < .05$) ค่าเฉลี่ยร้อยละของปริมาตรของช่องว่างระหว่างวัสดุและเนื้อฟันของกลุ่ม Biodentine/Blood ไม่มีความแตกต่างกับกลุ่ม MTA/Blood อย่างมีนัยสำคัญ ค่าเฉลี่ยร้อยละของปริมาตรของช่องว่างระหว่างวัสดุและเนื้อฟันของกลุ่ม Biodentine/NSS ต่ำกว่ากลุ่ม MTA/NSS อย่างมีนัยสำคัญทางสถิติ ($P < .05$) ค่าเฉลี่ยร้อยละของปริมาตรของช่องว่างระหว่างวัสดุและเนื้อฟันที่เวลาซึ่งตัวเริ่มแรกและที่เวลา 24 ชั่วโมงในแต่ละกลุ่มไม่มีความแตกต่างกัน ยกเว้นในกลุ่ม MTA/Blood ซึ่งพบว่าที่เวลา 24 ชั่วโมงมีค่าสูงกว่าที่เวลาซึ่งตัวเริ่มแรกอย่างมีนัยสำคัญทางสถิติ ($P < .05$) ค่าเฉลี่ยร้อยละของความพรุนของกลุ่ม Biodentine/Blood มีค่าสูงกว่ากลุ่ม Biodentine/NSS กลุ่ม MTA/Blood และกลุ่ม MTA/NSS อย่างมีนัยสำคัญทางสถิติ ($P < .05$) โดยค่าเฉลี่ยร้อยละของความพรุนของกลุ่ม Biodentine/NSS กลุ่ม MTA/Blood และกลุ่ม MTA/NSS ไม่มีความแตกต่างกัน ค่าเฉลี่ยร้อยละของความพรุนที่เวลาซึ่งตัวเริ่มแรกของวัสดุและที่เวลา 24 ชั่วโมงในแต่ละกลุ่มไม่มีความแตกต่างกัน ยกเว้นในกลุ่ม Biodentine/Blood ซึ่งพบว่าที่เวลา 24 ชั่วโมงมีค่าสูงกว่าที่เวลาซึ่งตัวเริ่มแรกอย่างมีนัยสำคัญทางสถิติ ($P < .05$) สรุปผลวิจัย: ภายใต้สภาวะปนเปื้อนเลือดไม่พบว่ามี ความแตกต่างของความแนบตามขอบกับเนื้อฟันระหว่างไบโอเด็นทีนและเอ็มทีเอ ในทางตรงข้ามสภาวะปนเปื้อนเลือดมีผลเพิ่มปริมาตรของช่องว่างระหว่างวัสดุและเนื้อฟันของวัสดุทั้งสองชนิด ไบโอเด็นทีนมีความพรุนมากกว่าเอ็มทีเอในสภาวะปนเปื้อนเลือดอย่างมีนัยสำคัญ ควรทำการห้ามเลือดอย่างเหมาะสมเมื่อใช้ไบโอเด็นทีนเป็นวัสดุซ่อมแซมรอยทะลุง่ามรากฟัน

ภาควิชา ทันตกรรมหัตถการ

ลายมือชื่อนิสิต

สาขาวิชา วิทยาเอ็นโดดอนต์

ลายมือชื่อ อ.ที่ปรึกษาหลัก

ปีการศึกษา 2558

5575817732 : MAJOR ENDODONTOLOGY

KEYWORDS: BIODENTINE / BLOOD CONTAMINATION / MARGINAL ADAPTATION / POROSITY / MICROCOMPUTED TOMOGRAPHY

RANGSIT MAKARUKPINYO: COMPARISON OF MARGINAL ADAPTATION TO DENTINE AND POROSITY OF BIODENTINE AND MTA IN BLOOD CONTAMINATED FURCATION REPAIR.
ADVISOR: ASST. PROF. DR. CHOOTIMA RATISOONTORN, Ph.D., 73 pp.

Introduction: This study compared the porosity and marginal adaptation to dentine of Biodentine and MTA in the presence and absence of blood in simulated furcation perforation cavities using micro-CT. Methods: Furcation perforation cavities were prepared on 64 extracted human mandibular first molars. Samples were randomly divided into 4 groups: Biodentine with blood contamination group (Biodentine/Blood), Biodentine with normal saline group (Biodentine/NSS), MTA with blood contamination group (MTA/Blood) and MTA with normal saline group (MTA/NSS). All samples were scanned using micro-CT at initial setting time and 24 hours. Mean percent gap volume was calculated from difference between cavity volume and material volume. Mean percent porosity obtained directly from the data report. Results: Blood contamination increased mean percent gap volume in both type of materials significantly ($P < .05$). Mean percent gap volume of Biodentine/Blood was not significantly different from MTA/Blood. Biodentine/NSS had significantly lower mean percent gap volume compared with MTA/NSS ($P < .05$). There was no significant difference in mean percent gap volume between initial setting time and 24 hours except for MTA/Blood, which showed significantly higher mean percent gap volume at 24 hours ($P < .05$). Biodentine/Blood had significantly higher mean percent porosity than Biodentine/NSS, MTA/Blood and MTA/NSS ($P < .05$). There was no significant difference in mean percent porosity between Biodentine/NSS, MTA/Blood and MTA/NSS. There was no significant difference in mean percent porosity between initial setting time and 24 hours except for Biodentine/Blood, which showed significantly higher mean percent porosity at 24 hours ($P < .05$). Conclusion: In blood contamination condition, there was no difference in marginal adaptation between Biodentine and MTA. Blood contamination significantly increased gap volume of both materials. In contrast, Biodentine had significantly higher porosity than MTA in blood contaminated condition. Appropriate hemostasis should be carried out when using Biodentine as a furcation repair material.

Department: Operative Dentistry

Student's Signature

Field of Study: Endodontology

Advisor's Signature

Academic Year: 2015

ACKNOWLEDGEMENTS

This thesis would have remained a distant dream for me, had it not been for several wonderful people. I would like to express my sincere gratitude to all of them.

First of all, it is with immense gratitude that I acknowledge the support and help of my thesis's advisor, Assistant Professor Dr. Chootima Ratisoontorn for guiding the whole thesis project with attention and care.

This thesis was supported by many people included Dr. Piyaporn Lalidwongsa, general dentist of Phachi hospital and Dr. Achariya Makarukpinyo, general dentist of Bangkruai hospital for their kindly help on teeth collection and patients' informed consent issue. I would like to thanks Dr. Nut Kulvanit of Department of Statistics, Faculty of Commerce and Accountancy, Chulalongkorn University for statistical analysis assistance and the staffs of Oral Biology Research Centre of Chulalongkorn University for their valuable laboratory assistance in this project. Moreover, I am grateful to Mr. Thammaroj Makarukpinyo for block and jig preparation for micro-CT scanning.

In this project, financial issue was partially supported by Chulalongkorn University Graduate School Thesis Grant.

Finally, I would like to take this opportunity to thank all thesis committees (Associate Professor Dr. Piyanee Panitvisai, Assistant Professor Dr. Anchana Panichuttra and Assistant Professor Dr. Jaruma Sakdee). Their kindly comments and guidance are greatly appreciated.

CONTENTS

	Page
THAI ABSTRACT	iv
ENGLISH ABSTRACT	v
ACKNOWLEDGEMENTS	vi
CONTENTS	vii
CONTENT OF FIGURE.....	1
CONTENT OF TABLES	1
CHAPTER I INTRODUCTION.....	1
Background and Rational.....	1
Objectives.....	3
Scope of study	4
CHAPTER II LITERATURE REVIEW	5
Root perforation.....	5
Mineral Trioxide Aggregate (MTA)	6
<i>Chemical properties</i>	6
<i>Physical Properties</i>	9
<i>Drawbacks of MTA</i>	10
Calcium chloride.....	11
Superplasticizer	12
Biodentine	13
<i>Chemical properties</i>	14
<i>Physical properties</i>	16
<i>Biodentine as perforation repair material</i>	18

	Page
Biocompatibility of perforation repair materials.....	19
Effects of blood contamination.....	20
Marginal adaptation.....	22
Microcomputed tomography (micro-CT).....	24
CHAPTER III RESEARCH METHODOLOGY	27
Target Population	27
Sample	27
Independent Variables.....	27
Dependent Variables.....	27
Control variables.....	27
Confounding Factors	27
Hypothesis.....	28
<i>Hypothesis 1</i>	28
<i>Hypothesis 2</i>	28
Ethical Consideration	28
Materials.....	28
Methods.....	30
<i>Teeth selection</i>	30
<i>Sample preparation</i>	30
<i>Perforation simulation</i>	34
<i>Cavity scanning for volume measurement</i>	34
<i>Blood contamination and material repair</i>	34
<i>Material scanning</i>	35

	Page
<i>Gap and porosity acquisition</i>	37
<i>Statistical analysis</i>	38
CHAPTER IV RESEARCH RESULTS	40
Percent gap volume.....	42
Percent porosity.....	46
CHAPTER V DISCUSSION.....	51
Limitations.....	57
Conclusion.....	58
REFERENCES	59
APPENDIX A Gap volume	69
APPENDIX B Porosity	71
VITA.....	73



CONTENT OF FIGURE

Figure 1: Hydration process of tricalcium silicate and the dicalcium silicate. (24)	7
Figure 2: Hydrated white Portland cement (SEM) (24).....	7
Figure 3: MTA particles (27)	8
Figure 4: Setting behavior of Biodentine (9).....	16
Figure 5: SEM micrograph of Biodentine after complete set. (9).....	17
Figure 6: (A) Tooth embedded into PVC ring; (B) A diagram showing alginate in the pulp chamber.....	31
Figure 7: After acrylic complete set, alginate was removed.	32
Figure 8: Roots removal using Isomet.....	32
Figure 9: Plastic jig ensured horizontal and vertical orientation of sample.	33
Figure 10: Index of a holder (a) and plastic jig (b) are used to stabilize horizontal orientation.....	33
Figure 11: Scout view screening of empty cavity and reference point setting.....	35
Figure 12: Scout view screening after perforation repair material was filled.....	36
Figure 13: Binary image (white: solid region, black: voids within the material, arrows: closed pores and open pores)	37
Figure 14: 3D reconstructive image of (A) cavity volume, (B) material volume. (C) Non-identical region of overlapped image demonstrated gap volume (arrows).	38
Figure 15: A Biodentine/Blood sample (A) 3D reconstruction of Biodentine and gap (arrows) at initial set; (B-D) random 2D images of internal 1/3, middle 1/3 and external 1/3, respectively. (H) 3D reconstruction of Biodentine and gap (arrows) at 24 hours; (E-G) random 2D images of internal 1/3, middle 1/3 and external 1/3, respectively. Black scatter within the material represents porosity.....	40
Figure 16: A Biodentine/NSS sample (A) 3D reconstruction of Biodentine and gap (arrows) at initial set; (B-D) random 2D images of internal 1/3, middle 1/3 and	

external 1/3, respectively. (H) 3D reconstruction of Biodentine and gap (arrows) at 24 hours; (E-G) random 2D images of internal 1/3, middle 1/3 and external 1/3, respectively. Black scatter within the material represents porosity. 41

Figure 17: A MTA/Blood sample (A) 3D reconstruction of MTA and gap (arrows) at initial set; (B-D) random 2D images of internal 1/3, middle 1/3 and external 1/3, respectively. (H) 3D reconstruction of MTA and gap (arrows) at 24 hours; (E-G) random 2D images of internal 1/3, middle 1/3 and external 1/3, respectively. Black scatter within the material represents porosity. 41

Figure 18: A MTA/NSS sample (A) 3D reconstruction of MTA and gap (arrows) at initial set; (B-D) random 2D images of internal 1/3, middle 1/3 and external 1/3, respectively. (H) 3D reconstruction of MTA and gap (arrows) at 24 hours; (E-G) random 2D images of internal 1/3, middle 1/3 and external 1/3, respectively. Black scatter within the material represents porosity. 42

Figure 19: Mean percent gap volume at initial set and 24 hours. I-bar represents standard errors. Double line and italic numbers represent mean percent gap volume of combined data of both time points. The same superscript letters were not significantly different of combined data of both time points (Mann-Whitney's U test, $P < .05$). * indicates significant difference between time points within groups (Wilcoxon signed rank test, $P < .05$). 43

Figure 20: Mean percent gap volume at (A) initial set and (B) 24 hours. I-bar represents standard errors. The same superscript letters were not significantly different (Mann-Whitney's U test, $P < .05$). 45

Figure 21: Mean percent gap volume at external 1/3, middle 1/3 and internal 1/3. I-bar represents standard errors. Double line and italic numbers represent mean percent gap volume of combined data of all 3 levels. The same superscript letters were not significantly different of combined data of all 3 levels (Mann-Whitney's U test, $P < .05$). * indicates significant difference between levels within group (Wilcoxon signed rank test, $P < .05$). 46

Figure 22: Mean percent porosity at initial set and 24 hours. I-bar represents standard errors. Double line and italic numbers represent mean percent porosity of combined data of both time points. The same superscript letters were not significantly different of combined data of both time points (Mann-Whitney's U test, $P < .05$). * indicates significantly difference between time points within groups (Wilcoxon signed rank test, $P < .05$). 47

Figure 23: Mean percent porosity at (A) initial set and (B) 24 hours. I-bar represents standard errors. The same superscript letters were not significantly different (Mann-Whitney's U test, $P < .05$). 49

Figure 24: Mean percent porosity at external 1/3, middle 1/3 and internal 1/3. I-bar represents standard errors. Double line and italic numbers represent mean percent porosity of combined data of all 3 levels. The same superscript letters were not significantly different of combined data of all 3 levels (Mann-Whitney's U test, $P < .05$). * indicates significantly difference between levels within group (Wilcoxon signed rank test, $P < .05$). 50

CONTENT OF TABLES

Table 1: Biodentine and MTA composition.....	14
Table 2: Mean percent gap volume (95% Confidence Interval for Mean) of combined data of both time points.....	44
Table 3: Mean percent porosity (95% Confidence Interval for Mean) of combined data of both time points.....	48
Table 4: Mean percent gap volume.	69
Table 5: Mean percent gap volume at initial set and 24 hours.	69
Table 6: Mean percent gap volume at external 1/3, middle 1/3 and internal 1/3.....	70
Table 7: Mean percent porosity.	71
Table 8: Mean percent porosity at initial set and 24 hours.	71
Table 9: Mean percent porosity at external 1/3, middle 1/3 and internal 1/3.....	72

CHAPTER I

INTRODUCTION

Background and Rational

Furcation perforation is one of the most common errors during root canal treatment and post space preparation which creates bacterial communication between root canal system and periodontal tissue. This could cause root canal system infection by periodontal bacteria, periodontal tissue infection by root canal bacteria or both, followed by endo-perio lesions which jeopardizes treatment outcome and prognosis of the tooth (1). The other concern of existence of communication is sodium hypochlorite accident during root canal irrigation. Therefore, immediate repair is needed to ensure the best prognosis.

Currently, Mineral Trioxide Aggregate (MTA) is the most popular furcation repair material due to its superior properties such as good biocompatibility (2, 3). However, MTA has disadvantage of very long setting time (4) and hence one-visit treatment was almost impossible. Many investigators are searching for permanent filling materials that can be placed over MTA without interfering with its setting properties for one-visit furcal perforation

repair. Nandini *et al.* (5) reported that placement of Glass Ionomer Cement (GIC) 45 minutes after placing White Mineral Trioxide Aggregate (WMTA) did not interfere with MTA setting and calcium salt was formed in the interface of both materials. Nonetheless, in some clinical situations such as inflammation, pus, bleeding or serum contamination can interfere with WMTA setting. In an inflamed environment, MTA is applied into acidic tissue condition. Saghiri *et al.* (6) found that lower pH compromised sealing ability of WMTA as a root-end filling material.

Recently, Septodont introduced a new dentine substitution material developed for many purposes such as dentine substitute under a composite filling, direct pulp capping material (7) and also as endodontic repair material. Biodentine (Biodentine™, Septodont, Saint Maur des Fossés, France) is a tricalcium silicate based material which reported to have biocompatibility similar to MTA and other Portland cements (8). However, Biodentine has only 6-12 minutes setting time (9) instead of 165 ± 5 minutes that is of MTA (4). From this outstanding advantage, Septodont claimed that Biodentine can be used as repairing material. However, long-term clinical success of this novel material has not yet been reported.

Perforations usually expose the periodontal tissue containing tissue fluid and blood. This could result in decreased sealing ability between repair material and dentine. Although the study by Chong *et al.* (10) showed that clinical success of MTA was satisfied, Maltezos *et al.* (11) reported that all materials showed leakage including MTA, the repairing material widely used nowadays. This leakage could affect long-term prognosis due to communication for bacterial transmission between root canal system and periodontal tissue. Sealing ability under blood contaminated circumstance of Biodentine, a new material claimed by manufacturer for good repair ability has not been studied. Therefore, this study aims to investigate the porosity and marginal adaptation of Biodentine in presence of blood contamination compared to MTA.

Objectives

The purpose of this study was to compare porosity and marginal adaptation to dentine of Biodentine and MTA in the presence and absence of blood in simulated furcation perforation cavities using microcomputed tomography (micro-CT).

Scope of study

This *in vitro* study was performed in simulated perforation cavity on human teeth. Micro-CT was used to measure perforation cavity volume, repair material volume and porosity of repair material. Marginal adaptation was undertaken as gap volume which was calculated from the difference between cavity volume and material volume.

As previously mentioned, superior property of Biodentine is shorter setting time which could decrease number of dental visits, while it can maintain other beneficial properties of MTA. The results of this study will help elucidating the potential of Biodentine as an alternative to MTA in perforation repair by comparing marginal adaptation and porosity of Biodentine to MTA in blood contaminated condition. Porosity relates with mechanical properties of materials (12). This will elucidate whether of blood contamination in perforation affects material properties.

CHAPTER II

LITERATURE REVIEW

Root perforation

Root perforation is an artificial communication between root canal system and supporting tissues of teeth or oral cavity (13). Often these situations occur iatrogenically from misdirection of instrumentation especially from rotary instruments e.g. burs, Gates Glidden drills, during access preparation, canal localization (14), negotiation of curved canal, strip perforation on danger zone (15) and post space preparation.

Root perforation is one of the causes of endodontic failure (16). Recent study reported that perforations played part in mid-treatment complications which decrease success rate from 84% to 69% in conventional cases (17) and 87% to 56% in retreatment cases (18). Prognosis is based on factors contributing to prevention and cessation of bacterial transmission at the perforation sites including location, size, timing to closure of perforation and sealing ability of repair materials (13, 19, 20). Early detection and repair prevent breakdown of periodontium and further formation of endo-perio lesion which could complicate prognosis. Furthermore, good bacterial control and adequate seal

play important role on long-term prognosis. Proper selection of repair material is also influence the prognosis despite early detection and immediate closure. Materials used for reparation are amalgam, Glass Ionomer (19), IRM, Super EBA and MTA . Currently, MTA is the most generally accepted furcation repair material because of its physical properties and biocompatibility (21).

Mineral Trioxide Aggregate (MTA)

MTA composition is similar to Portland cement used in construction industry except for bismuth oxide. MTA had been first introduced in dentistry by Torabinejad in 1993 (22) and gain popularity in endodontics especially for repairing propose due to its superior properties; good sealing ability, biocompatibility (22), ability to set in moisture (4), induce periodontal repair and cementogenesis (23).

Chemical properties

MTA sets through hydration process (figure 1). When tricalcium silicate and/or dicalcium silicate particles react with water, it will form nanoporous amorphous calcium silicate hydrated (CSH) gel ($\text{CaO} \cdot 2\text{SiO}_2 \cdot 3\text{H}_2\text{O}$) which increase to the saturation point surround non-reacted molecule. Calcium hydroxide (CH) ($\text{Ca}(\text{OH})_2$) crystals are also formed and fulfil CSH gel porosity as it grows stronger

(24). Owing to formation of calcium hydroxide, MTA has high alkalinity after hydration which resulted in its anti-microbial activity. Because of hydration reaction, MTA is considered hydrophilic (4).

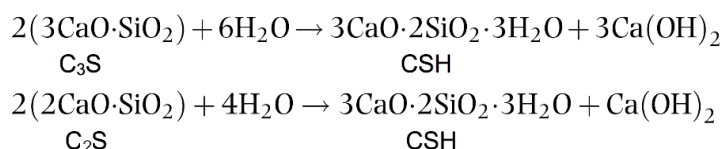


Figure 1: Hydration process of tricalcium silicate and the dicalcium silicate.

(24)

Camilleri *et al.* (24) studied cured WMTA cement. They founded that *in situ* hydrations product of calcium silicate hydrate (ip) and unhydrated residual of cement (bright grains) was confined within original particle bound surrounded by undifferentiated product of calcium silicate hydrate (op) and calcium hydroxide (CH, white amorphous) which area was originally occupied by water when the paste was first mixed (figure 2).

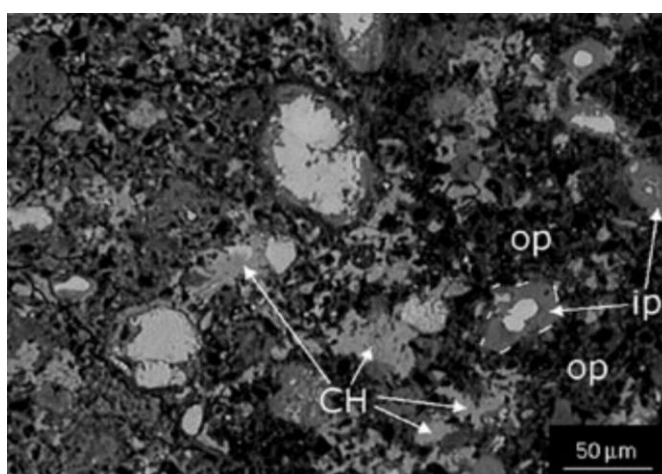


Figure 2: Hydrated white Portland cement (SEM) (24).

There are many studies about MTA chemical composition. Parirokh and Torabinejad (4) reviewed comprehensively on these studies and suggested that results of chemical composition of MTA are varied may be due to differences in equipment or preparation criteria used in experiments (such as different liquid used (25)). Two types of MTA are mainly in the market; Gray Mineral Trioxide Aggregate (GMTA) and White Mineral Trioxide Aggregate (WMTA). Both of them contains tricalcium silicate and bismuth oxide but GMTA contains higher amount of dicalcium silicate and more iron, aluminum and magnesium than in WMTA (26). Cement particle size is varying between $<1\ \mu\text{m}$ and $50\ \mu\text{m}$ (average $30\ \mu\text{m}$). Bismuth oxide particle size is around $10\text{--}30\ \mu\text{m}$ (24).

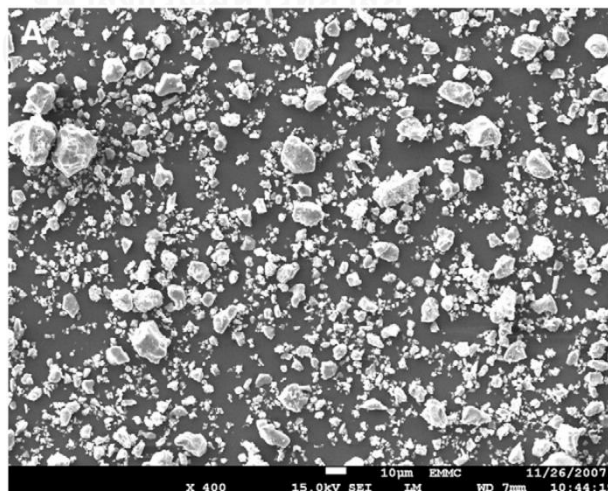


Figure 3: MTA particles (27)

Physical Properties

Setting time, porosity, flexural and compressive strength, micro-hardness, bonding to materials, expansion and solubility of MTA have been extensively studied. Several factors influence MTA's physical properties. These factors are water-to-powder ratio (28), environment humidity (29), pH (6), mixing method (4) and condensation method (30).

MTA setting time is about 165 ± 5 minutes in the water-to-powder ratio of 1:3, which is the manufacturers' recommendation for clinical uses (28). Islam *et al.* (31) reported initial setting time of WMTA was 40 ± 2.94 minutes and GMTA was 70 ± 2.58 minutes and final setting time of WMTA was 140 ± 2.58 minutes and GMTA was 175 ± 2.55 minutes. GMTA has higher amount of dicalcium silicate, which has slower hydration rate (32). This could explain longer setting time of GMTA compared with WMTA.

Torabinejad *et al.* (33) founded that compressive strength of MTA is significantly lower than amalgam, IRM, Super EBA in the first 24 hours, but there is no different from IRM or Super EBA after 3 weeks. Solubility rate of MTA was found to be high in the first observation day, but it decreased exponentially in the 1, 3, 4, 5, 7, 9, 20 and 28 days (34). Porosity was found to be related with

amount of water (35), air entrapment (36, 37) and acidic pH value (12). By increasing of these factors will increase porosity of MTA.

Chng *et al.* (38) found MTA has setting expansion, in particular WMTA has greater setting expansion than GMTA. This could explain high sealing ability of MTA when compare with other materials. Torabinejad found that MTA has no apparent visible gap whereas amalgam, super EBA and IRM present gaps sized 4.8 ± 5.65 , 6.31 ± 5.57 and 8.37 ± 4.61 micron, respectively (39).

Drawbacks of MTA

The drawbacks of MTA include long setting time, discoloration potential, presence of toxic elements in the material composition, water-to-powder ratio is sensitive to material properties, difficulties on manipulation and application, high material cost, absence of a known solvent. MTA removal after setting is difficult (40).

Cavenago *et al.* (28) found that water-to-powder ratio significantly affected MTA (white MTA Angelus) physically and chemically. More powder was more radiopacity, lower setting time, lower pH and lower solubility. Fridland and Rosado (35) studied MTA solubility in 78-day period found that MTA solubility was highest at the beginning. Higher water-to-powder ratio increase

solubility at all time points (1, 2, 5, 9, 14, 21, 30, 50 and 78 days). Mixing MTA manually cannot archive optimum ratio in every mixing.

Setting time is the biggest concern of clinical uses. Dentists cannot continue their work instantly after applying MTA. Although literature suggested that GIC can be placed over MTA after 45 minutes (5), ~~but~~ ideally MTA setting should be confirmed and MTA should be replaced in case of incomplete setting (41).

Many researchers are trying to overcome these drawbacks of MTA. Many additives are added to improve MTA properties. Calcium chloride was used to reduce setting time (42). Superplasticizer was used to decrease water portion in the mixture to improve physical properties (43). Pre-capsulation of the mixture was done for ease of manipulation. Purity of mixture was to control setting reaction.

Calcium chloride

In construction industry, calcium chloride is added into Portland cement as hydration process accelerator (42). This is also applied to dental Portland cement (44). Acceleration of CSH crystal formation by calcium chloride is dose dependent. Calcium chloride increases ionicity which promotes

crystallization (42). Calcium chloride concentration at 15% reduced initial setting time from 90 minutes to 50 minutes and 180 minutes of final setting time to 90 minutes. At 20% of concentration initial setting time and final setting time increased to 85 and 130 minutes, respectively. Structural porosity reduced as concentration of calcium chloride increased and reached maximum density at 10% concentration. However, porosity increased as concentration of calcium chloride increased beyond 15%. X-Ray Diffraction (XRD) analysis found that increased concentration of calcium chloride reduced calcium hydroxide originated from the reaction and lowered pH from 11 to 10.5 at 48 hours. Maximum compressive strength is also increased 4 times at 10% calcium chloride concentration then began to decrease with a further increase in calcium chloride concentration beyond 10%. (44)

Superplasticizer

Superplasticizer, a water-reducing agent, enhances precipitation process. Superplasticizer, acts as surfactant, creates negative charge on surface of cement particles. From this mechanism, particles were dispersed allowing water molecules to surround them easily and gives better wet-ability of

material. Adding of polycarboxylate superplasticizer into Portland cement will increase flowability significantly and dose-dependently (43).

From MTA's drawbacks, several materials were developed and launched into the market to fulfil ideal repair material properties such as Biodentine (Septodont), CEM cement (BioniqueDent), Biosealer (Isasan), DiaRoot and BioAggregate (Innovative BioCeramik). Biodentine is the material of interest for this study as a furcation repair material because of its properties and availability in Thailand.

Biodentine

Biodentine was invented by Septodont, France. Biodentine is considered as a calcium silicate based material which is the same as MTA. MTA and other silicate based materials are derived from natural Portland cement which are not purified. Those materials are composed of dicalcium silicate (C_2S , $2CaO.SiO_2$) and tricalcium silicate (C_3S , $3CaO.SiO_2$), tricalcium aluminate ($3CaO.Al_2O_3$), calcium aluminoferrite ($4CaO.Al_2O_3.Fe_2O_3$), calcium sulphate ($Ca(SO)_4$ or gypsum) and other metal compounds. Septodont researchers attempted to make purified calcium silicate material by using active biosilicate

technology to control manufacturing process. This new material is pre-proportionally measured and delivered pre-capsulated.

Table 1: Biodentine and MTA composition

Biodentine composition (9)	
<i>Powder</i>	<i>Liquid</i>
Tricalcium silicate ($3\text{CaO}\cdot\text{SiO}_2$) - Main core material	Water
Dicalcium silicate ($2\text{CaO}\cdot\text{SiO}_2$) - Second core material	Calcium chloride (CaCl_2) - Accelerator
Calcium carbonate and oxide (CaCO_3 , CaO) - Filler	Polycarboxylate hydrosoluble polymer –
Iron oxide (Fe_2O_3) - Shade	Water-reducing agent
Zirconium oxide (ZrO_2)- Radiopacifier	
MTA composition (45)	
<i>Powder</i>	<i>Liquid</i>
Tricalcium silicate ($3\text{CaO}\cdot\text{SiO}_2$)	Water
Dicalcium silicate ($2\text{CaO}\cdot\text{SiO}_2$)	
Tricalcium aluminate ($3\text{CaO}\cdot\text{Al}_2\text{O}_3$)	
Tetracalcium aluminoferrite ($4\text{CaO}\cdot\text{Al}_2\text{O}_3\cdot\text{Fe}_2\text{O}_3$)	
Calcium sulfate dihydrate ($\text{CaSO}_4\cdot 2\text{H}_2\text{O}$)	
Calcite, bismuth oxide (Radiopacifier), alkali metal oxides (CaCO_3 , Bi_2O_3 , CaO , MgO)	
Alkali metal sulfates (K_2SO_4 , Na_2SO_4)	

Biodentine consists of liquid and powder components. The composition of powder and liquid is shown in table 1. Core particle in the powder will react with the liquid only on the surface of the particle to form CSH gel surrounding non-react particles as shown in figure 5.

Chemical properties

Setting reaction of Biodentine is hydration process, similar to others silicate based materials. This also made Biodentine hydrophilic. Tricalcium silicate or Dicalcium silicate react with water to form nanoporous amorphous

CSH gel which increase to the saturation point surround non-reacted molecule along with calcium hydroxide crystal filling CSH gel porosity.

Biodentine was made purified. Products are free of aluminate, sulphate, or ferrate. Particle size was controlled. Although Septodont (9) claimed the purity of Biodentine yielded from 2 main components, tricalcium silicate and dicalcium silicate. Camilleri *et al.* (46) reported that only tricalcium silicate was detected in Biodentine and no calcium oxides were found in the mixtures.

Faster setting time depends on smaller particle size (more reacted surface), having calcium chloride as accelerator and lesser liquid contents. Hydrosoluble polymer, water-reducing agent, is added into mixtures to reduce viscosity during mixing (47). The material contains lesser water without compromising mixture characteristic. With minimal water, porosity is also minimized (35). Moreover, removing gypsum could significantly reduce setting time (48).

In conclusion, Biodentine have been chemically improved by removing of gypsum and adding of calcium chloride as accelerator resulted in fast setting. Rapid setting reaction can be controlled by using of superplasticizer which make material more workable.

Physical properties

Calcium silicate of Biodentine is synthesized under Active Biosilicate Technology concept. Calcium silicate of MTA is naturally derived from Portland cement. Biodentine is composed of purified material to control mechanical strength and shorter the setting time to overcome MTA drawbacks. Biodentine gives sufficient mechanical resistance to be used as a dentine substitute. From its purity and homogeneity particles, setting time was reduced. Setting time of Biodentine is about 9-12 minutes (9).

Adding of calcium carbonate into the formulae also helps create nucleation site for CSH, reducing the duration of the induction period so initial setting could be expected after a few minutes (49).

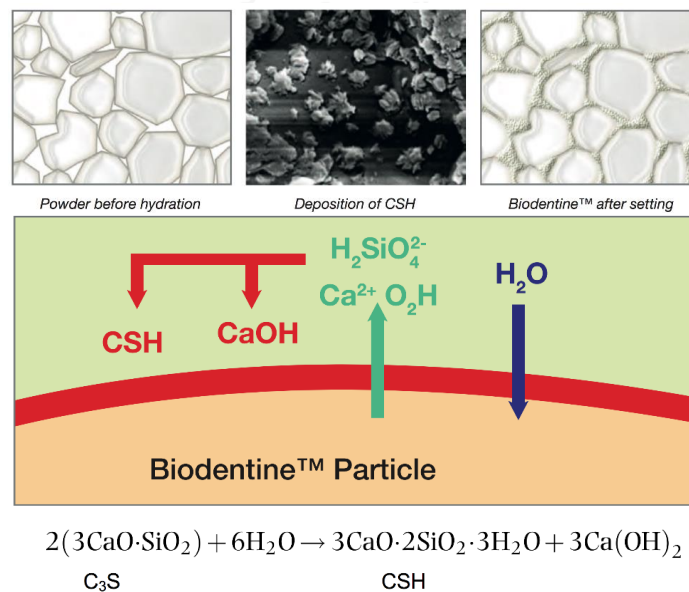


Figure 4: Setting behavior of Biodentine (9).

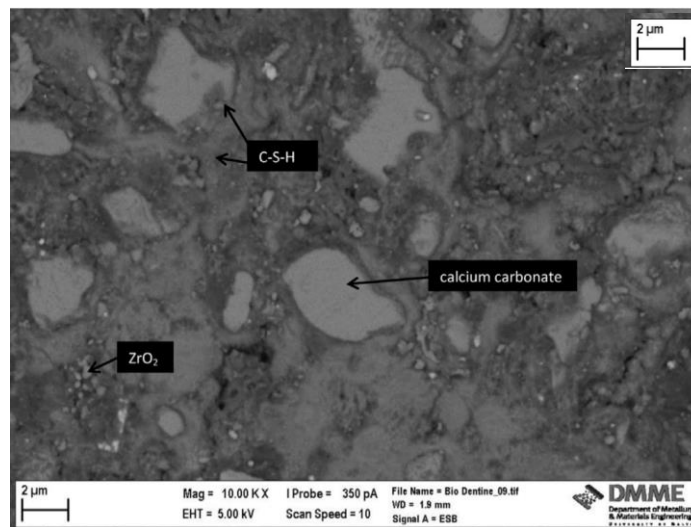


Figure 5: SEM micrograph of Biodentine after complete set. (9)

Advantage of purification is remarkable on reduction of setting time.

Camilleri *et al.* (50) and Wongkornchaowalit and Lertchirakarn (43) found that excluding gypsum from the cement reduced setting time significantly.

Superplasticizer, improves consistency and flowability of Biodentine, improves application and flowability into dentinal tubules (9), increases compressive strength, which resulted from lower water-to-powder ratio and decrease of porosity, gives 300 mPa which is about to dentine. Reduction of exothermic process during hydration process reduce shrinkage which leads to leakage (43).

Septodont claimed that MTA did not develop any mechanical resistance even after 1 day. Compressive strength reached half of dentine in 7

days, approximately 150 mPa. On the other hand, Biodentine yielded 100 mPa within the first hour and after 7 days, its mechanical resistance reached 250 mPa, almost equal to dentine (9).

Porosity of Biodentine was tested by manufacturer using mercury intrusion porosimetry at 28 days after mixing. Density and porosity of Biodentine is not difference from Fuji IX, but less porosity than MTA. Moreover, testing by electrochemical impedance spectroscopy found that after initial setting porosity will decrease (9).

Adding zirconium oxide radiopacifier instead of bismuth oxide, calcium chloride as accelerator, superplasticizer as water-reducing agent giving better compressive strength, solubility and porosity, and capsulation for ease of manipulation are the major changes to improve physical properties of this novel material.

Biodentine as perforation repair material

Guneser *et al.* (51) found that Biodentine was suitable for perforation repair regardless to contamination of various types of irrigant and also found that Biodentine gives higher push-out bond strength than that MTA does.

Biodentine showed considerable performance as a perforation repair material even after being exposed to various endodontic irrigant.

Biocompatibility of perforation repair materials

Perforation repair materials usually contact with periodontium. There are *in vitro* (52) and *in vivo* (53) experiments to assess the biocompatibility of dental materials. A study on human periodontal ligament (PDL) cell cultures compared MTA with amalgam and Super EBA indicated that freshly mixed MTA has lower cytotoxicity potential than Super EBA or amalgam (52). Twenty-four hours after mixing at a higher extract concentration, MTA showed the least amount of cytotoxicity of all the tested materials; at a lower extract concentration, Super EBA showed higher cytotoxicity than amalgam or MTA. MTA is not mutagenic (54) and non-neurotoxic (55) and does not produce a side effect on microcirculation (56). Recent study suggested that MTA has vasoconstrictor property and hemorrhage control, which is critical for the success of pulp-capping treatment (57).

Biocompatibility of Biodentine found to be similar to MTA. *In vitro* study reported that Biodentine and MTA were less cytotoxic than glass ionomer (58). Hard tissue induction properties of MTA were also noted in Biodentine (8).

Hydroxyapatite structure was reported in 2 days and osteodentine in 14 days (59). Dentin bridges from Biodentine and MTA in a human study were thick and homogeneous with minimal tunnel defects (60).

Recently, clinical Biodentine application in endodontics is only reported by the manufacturer such as direct pulp capping, Cvek's pulpotomy, complete pulpotomy, traumatic pulp exposure, perforations repair, retrofilling, primary teeth pulpotomy and apexification. Success of these applications was also only claimed by the manufacturer (9).

Effects of blood contamination

In the majority of endodontic applications, MTA might come into contact with blood during placement. Blood contamination of MTA resulted in a lack of acicular crystals, which can explain the reduction in compressive strength. Nekoofar *et al.* (41), Jasicki & Zielinski (36) demonstrated the air entrainment effect of red blood cells when mixed with Portland cement. Many small air bubbles are incorporated into concrete and become part of the matrix, resulting in increasing of porosity.

Vanderweele *et al.* (25) evaluated the resistance to displacement of WMTA in blood contaminated condition in various of liquid mixed. These

liquids included; water, anesthetic agent, normal saline. MTA resistance to fractures reduced in blood contaminated condition regardless of liquid used. Bonding failure between MTA and dentine was adhesion failure (MTA and dentine). There will be a decrease in the retention of MTA in the perforated furcal area in the presence of blood no matter various types of liquids secondary contaminated.

Kayahan *et al.* (61) and Namazikhah *et al.* (12) mentioned about acidic condition and blood contaminated condition leads to lack of acicular crystals which resulted in lower of compressive strength and hardness, respectively. Remadnia *et al.* (62) found that blood increased porosity in Portland cement and decreased compressive strength resulted from air entrainment effect.

Blood contamination is a cause for encountering unset MTA at a subsequent evaluation appointment. If MTA remains unset, it, ideally, should be replaced. This is one of the most important disadvantages of MTA (41). Although it was shown that MTA is leaked but its leakage is significantly less than other materials, either in the presence or absence of blood (63).

Marginal adaptation

There were many studies concluded that marginal adaptation is importance in the success of periradicular surgery (64-66) and sealing ability of perforation repair material to perforated sites is vital to prognosis of perforated teeth (19).

Terms of marginal adaptation has not been clearly described. Peter and Peter (65) categorized marginal adaptation into 2 categories. First is continuous margin which there is no gap visible between root-end cavity wall and filling material no matter what it is under-filled or overfilled Second is non-continuous margin where there is gap apparent between root-end cavity wall and filling material. This study was done by scanning electron microscopic (SEM) methods.

Correlation was established between marginal adaptation and seal ability in the several studies. From Shani *et al.* (67), radioisotope $10 \mu\text{Ci } ^{22}\text{Na}$ infiltration penetration was used for evaluation of seal ability of retrograde filling materials. This study showed that amalgam has significantly higher infiltration than Duralon, Cavit-W, zinc phosphate cement and Restodent. The study of Stabhotz *et al.* (64), an SEM study, was focusing on marginal

adaptation. Amalgam had the greatest gap size at 30 μm . Duralon and Cavit-W had the gap size between 8-15 μm . Zinc phosphate cement and Restodent had 5 μm and 1 μm gap size respectively.

Many methods are used to assess marginal adaptation. The methods include SEM, bacterial leakage, methylene blue dye. Torabinejad *et al.* (39) compared marginal adaptation of amalgam, Super EBA, IRM and MTA by using 4-point gap size measurement under SEM found that gap sizes were 4.8 ± 5.65 , 6.31 ± 5.57 , 8.37 ± 4.61 micron and no visible gap, respectively.

From a bacterial leakage study using *Staphylococcus epidermidis* to penetrate a 3-mm thickness of amalgam, Super EBA, IRM and MTA as root-end filling materials Whereas MTA did not show any leakage throughout 90 days' experimental period but majority of other samples began to leak at 6-57 days. (68) Recent methylene blue penetration studies showed 12 to 28 μm gap size between amalgam and dentinal wall in clinically root-end filled extracted teeth (63, 69). These studies indicated that MTA has good adaptation when compared with other root-end filling materials.

Sanghvi *et al.* (70) studied sealing ability of MTA, Biodentine and calcium phosphate cement as a furcal perforation repair material using methylene blue

penetration methods. Result given indicted that Biodentine has intermediated level of anti-leakage property inferior to MTA.

Microcomputed tomography (micro-CT)

In the past, conventional radiography was limited to providing only 2-dimension (2D) image that represent the summation of material attenuation along the x-ray path. Computed tomography (CT) had been introduced since 1970s. This is an advance of diagnosis imaging revolutionary. Its procedure makes up with collection of multiple viewing angles and reconstructs them to produce 3-dimension (3D) spatial distribution maps of material density within attenuating material and tissue including teeth. In contrast to 2D imaging, CT provides 3D reconstructive image which is composed of 1-mm^3 volume elements (voxel) (71).

In the early 1980s, micro-CT had been introduced with much better spatial resolution. It provides smaller voxel size, 5-50 microns, approximately 1 million times smaller than CT. Micro-CT system using microfocal spot X-ray sources and high resolution detectors, allow for projections rotated through multiple viewing directions to produce 3D reconstructive image of samples. The images represent spatial distribution maps of linear attenuation coefficients

determined by the energy of the X-ray source and the atomic composition of the material sample (71).

Normally section method is a gold standard of marginal adaptation assessment. Disadvantages and limitations of sectioning method are that some tissues disappear when the sections are cut, it provides only a limited number of sections, it is a destructive method. In contrast micro-CT can produce continuous image acquisition, gives unlimited number of sections and it is a non-destructive method (72). Swain and Xue (71) reviewed that micro-CT provides a noninvasive method to study of enamel thickness and tooth measurement, analysis of root canal morphology, evaluation of root canal preparation, craniofacial skeletal development and structure, biomechanics, tissue engineering, mineral concentrations of teeth and implant and peri-implant bone. A study by Fridland and Rosado (34) showed that freshly mixed MTA has significant solubility within initial setting period. Sample preparation using section method is impossible. Micro-CT scanning is non-destructive method which does not interfere with initial setting of MTA.

Micro-CT was used widely in biomedical research for bone and teeth inspection (73) and structure analysis of scaffolds for tissue engineering

application (74). It was also used in combination with other method for inspections of mineral concentration level of teeth. Sun *et al.* (75) used micro-CT to study polymerization shrinkage and leakage assessments of resin composite (76) and found that microleakage could be evaluated by 3D micro-CT reconstructive image analysis and agreed well with those obtained by dye penetration. Al-Fouzan *et al.* (77) studied effect of acid etching on marginal adaptation of mineral trioxide aggregate to apical dentine. This study found that micro-CT could measure gap volume between MTA and dentin. Gap volume measured were $0.00596 \pm 0.002 \text{ mm}^3$ and $0.00366 \pm 0.001 \text{ mm}^3$ for WMTA and Etched-WMTA, respectively. No significant difference in gap volumes between WMTA and Etched-WMTA. Gap volumes of GMTA was $0.0536 \pm 0.002 \text{ mm}^3$ and Etched-GMTA was $0.00716 \pm 0.004 \text{ mm}^3$. Significant differences in the gap volumes between GMTA and Etched-GMTA were found at p-value < 0.001.

Therefore, micro-CT seems to be a valid tool for studying porosity and marginal adaptation of repair material to dentin in perforation repair. It can provide non-destructive investigation of incomplete set materials.

CHAPTER III

RESEARCH METHODOLOGY

Target Population

Perforation cavities on furcation

Sample

Human lower mandibular molars with simulated furcation perforation cavity

Independent Variables

Blood contamination

Material

Time observed

Dependent Variables

Gap volume and porosity



Control variables

Volume of blood and normal saline, water-powder-ratio of the materials

Confounding Factors

Human error from perforation cavity preparation, pressure used for material application

Hypothesis

Hypothesis 1

Ho: In blood contaminated condition, gap volume between dentin wall and Biodentine is not different from between dentin wall and MTA

Ha: In blood contaminated condition, gap volume between dentin wall and Biodentine is different from between dentin wall and MTA

Hypothesis 2

Ho: In blood contaminated condition, porosity of Biodentine is not different from MTA

Ha: In blood contaminated condition, porosity of Biodentine is different from MTA

Ethical Consideration

Ethical issue was approved by Research Ethics Committee of Faculty of Dentistry, Chulalongkorn University (HREC-DCU 2014-017) because of using extracted human teeth and human blood.

Materials

1. Slow-speed diamond saw (Isomet; Buehler, Lake Bluff, IL, USA)
2. No.1.2 round diamond bur
3. No.5 Gates Glidden drill (Dentsply, Maillefer, Ballaigues, Switzerland)

4. 1.2-mm diameter MTA applicator (Angelus Soluções Odontológicas, Londrina, Brazil)
5. SCANCO μ CT35, micro-CT scanner (SCANCO Medical AG)
6. Humidity chamber
7. 2-20 μ L scale auto-pipette (Glassco, UK)
8. Scotch[®]tape (3M, MN, USA)
9. 64 human mandibular molars
10. Biodentine (Biodentine[™], Septodont, Saint Maur des Fossés, France)
11. MTA (ProRoot[®]MTA, Dentsply/Tulsa Dental, Tulsa, OK)
12. 0.1% Thymol solution
13. 20-mm diameter, 1-cm high PVC ring
14. Alginate
15. Self-cured acrylic resin
16. Human blood (The Thai Red Cross Society)
17. Normal saline solution
18. Distilled water
19. 27-gauge irrigate syringe with disposable syringe

20. CollaTape® (Sulzer Calcitek Inc., Carlsbad, CA)

21. Celluloid strips

Methods

Tooth samples were acquired from consented patients who undergone extraction for therapeutic reasons (e.g. periodontal reasons, caries). Blood was acquired from The Thai Red Cross Society.

Teeth selection

Sixty-four human mandibular molars were used in this study. Teeth must have at least 1.5 mm of thickness, intact furcation area without caries or cervical root caries, no previous root canal treatment. All teeth were stored in 0.1% thymol solution after extraction.

Sample preparation

Access opening was performed in order to expose pulpal floors. Furcation thickness measured by metal gauge to ensure at least 1.5 mm of thickness.

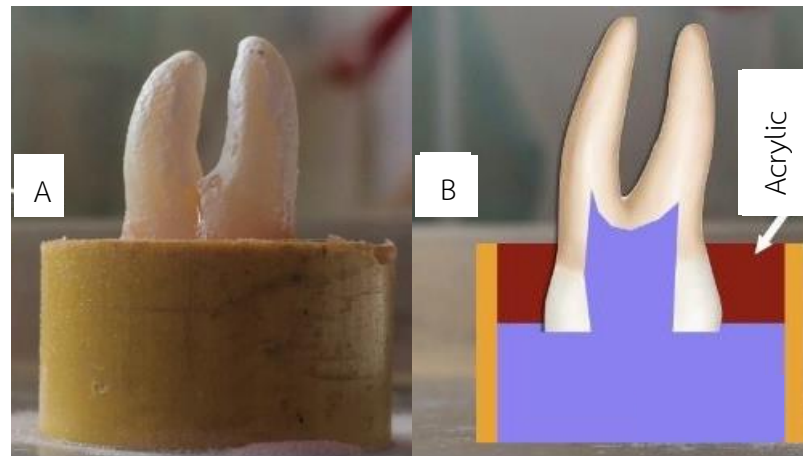


Figure 6: (A) Tooth embedded into PVC ring; (B) A diagram showing alginate in the pulp chamber.

The pulp chamber was filled with alginate before embedded upside down into 20-mm outer diameter PVC rings modified from the water pipe using self-cured acrylic resin (figure 6). Alginate which occupied access to pulpal floor, was removed after acrylic setting to provide clear access to floor of pulp chamber (figure 7). Roots were removed by precision slow-speed diamond saw (Isomet; Buehler, Lake Bluff, IL, USA) at the level of furcation (figure 8) result in flat furcation surface. Orientation jig was fabricated to ensure horizontal orientation of the samples in the holder during scanning. (figure 9, 10).



Figure 7: After acrylic complete set, alginate was removed.

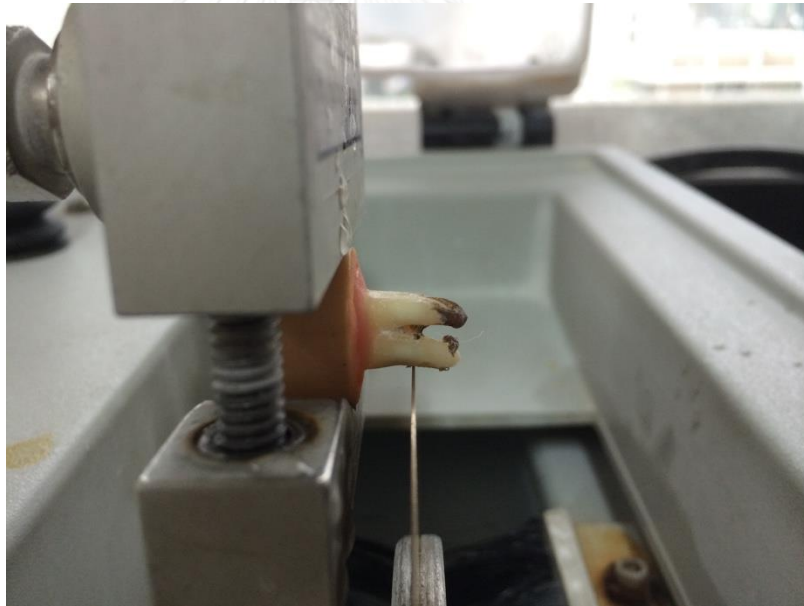


Figure 8: Roots removal using Isomet.



Figure 9: Plastic jig ensured horizontal and vertical orientation of sample.

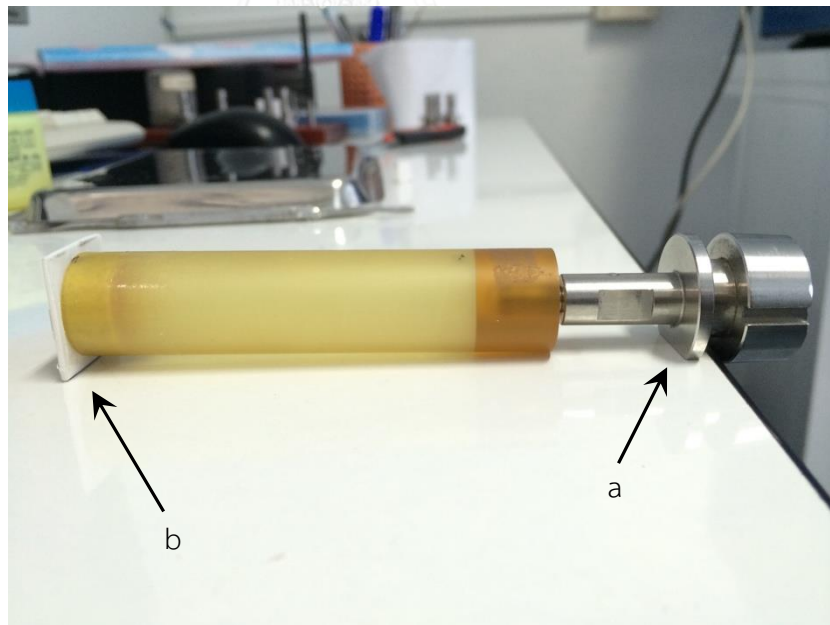


Figure 10: Index of a holder (a) and plastic jig (b) are used to stabilize horizontal orientation.

Perforation simulation

Furcation perforation procedure was modified from Rahimi *et al.*, (78). Briefly, by using a No. 1.2 round diamond bur perpendicular to the furcal floor and parallel to block axis and enlarged to a diameter of 1.3 mm with a single active penetration of No. 5 Gates Glidden drill (Dentsply, Maillefer, Ballaigues, Switzerland).

Cavity scanning for volume measurement

Cavity volume was measured by SCANCO μ CT35, micro-CT scanner (SCANCO Medical AG) at 70 kVp source voltage, 114 μ A, 8W source current, high resolution and 10-micron voxel size. One hundred and fifty consecutive slices of each sample were chosen, resulting in a 1.5-mm high volume of interest (VOI) of cavity volume.

Blood contamination and material repair

Samples were divided into 4 groups as follows: Biodentine with blood contamination group (Biodentine/Blood), Biodentine with normal saline group (Biodentine/NSS), MTA with blood contamination group (MTA/Blood) and MTA with normal saline group (MTA/NSS).

In blood contaminated groups, furcation surfaces of the samples were faced down on glass slab lining with 4x4 mm CollaTape soaked with 5.6 μ l of

blood. Material was mixed according to manufacturers' instructions and placed in the furcal cavities using a 1.2-mm diameter MTA applicator (Angelus Soluções Odontológicas, Londrina, Brazil). Moist cotton pellets were placed over repair materials followed by plastic covers to prevent desiccation.

In groups without blood contamination, normal saline solution was used instead of blood. The rest of the procedural steps were similar to those in the blood contaminated groups.

Material scanning

All samples went through scout view screening (figure 11) before scanning initiation. Scout view screening after filling with perforation repair material was used for initial inspection of material (figure 12).

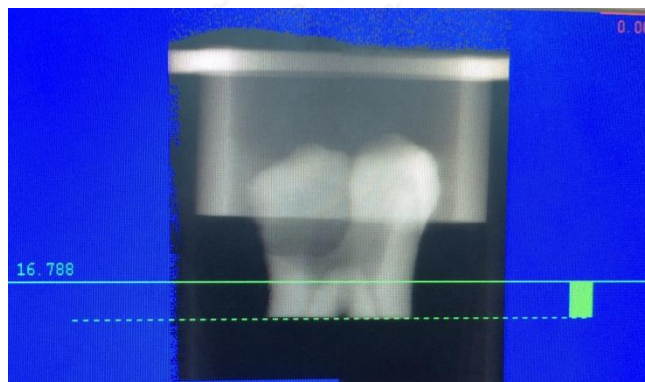


Figure 11: Scout view screening of empty cavity and reference point setting.

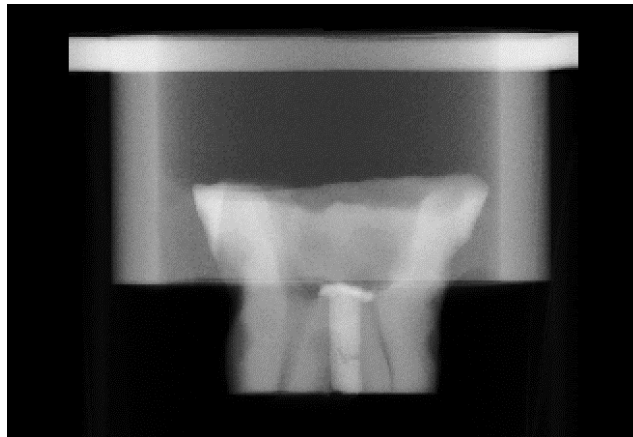


Figure 12: Scout view screening after perforation repair material was filled.

For scanning at initial set, only 2 slots of scanner were used. The first slot was for Biodentine groups and the second slot was for MTA groups. The first slot started scanning at 6 minutes which is the initial setting time of Biodentine. It required 37 minutes to complete a scan before initiation of scanning second slot which contained MTA samples. MTA has approximately 45 minutes initial setting time.

Exposure and settings were set as described above. Scanned samples were kept for 24 hours in 100% humidity, 37°C. After 24 hours, micro-CT scanning was repeated in the same pattern. Data were collected. Cavity volume, material volume and material porosity were obtained.

One hundred and fifty consecutive slices of each sample were chosen, resulting in a 1.5-mm high volume of interest (VOI). Semi automatically drawn

contours were generated according to radiodensity to define a mask for the barrier VOI of material mass. Radiodensity was adjusted until optimum radiodensity was obtained, making cross-sectional greyscale radiographic image mimic binary image (figure 13). Only closed porosity (pores with no contact with the material external surface) was included to be porosity, open pores (pores contact with the material external surface) was excluded as shown in figure 13.

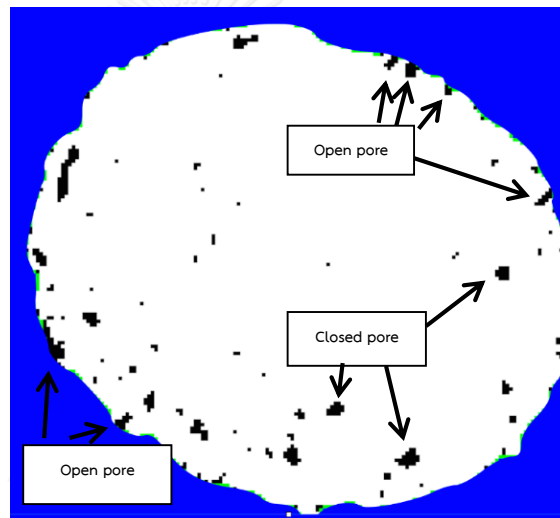


Figure 13: Binary image (white: solid region, black: voids within the material, arrows: closed pores and open pores)

Gap and porosity acquisition

3D reconstructive data provided cavity volume (mm^3) (figure 14A), material volume (mm^3) at initial set and 24 hours (figure 14B) and percent porosity of material at initial set and 24 hours. Percent porosity obtained

directly from the data report. Conversely, percent of gap volume had to be calculated indirectly (figure 14C) by following formula;

$$\text{Percent gap volume} = \frac{\text{Cavity Volume (mm}^3\text{)} - \text{Material Volume (mm}^3\text{)}}{\text{Cavity Volume (mm}^3\text{)}} \times 100$$

In addition, 3D data of each sample was divided into three levels of 0.5-mm thickness as follows: external 1/3 (0.01-0.50 mm, contact with blood or NSS), middle 1/3 (0.51-1.00 mm) and internal 1/3 (1.01-1.50 mm) (figure 14).

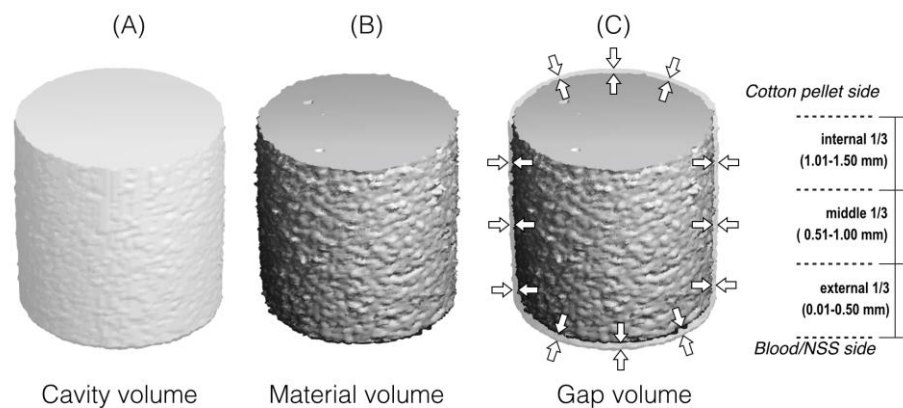


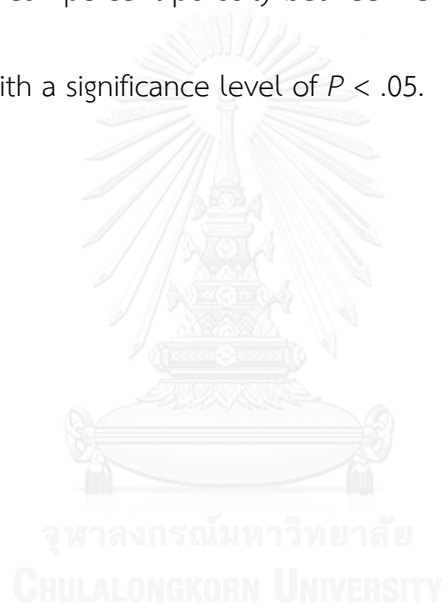
Figure 14: 3D reconstructive image of (A) cavity volume, (B) material volume. (C) Non-identical region of overlapped image demonstrated gap volume (arrows).

Statistical analysis

The data were analyzed using Statistical Package for Social Science (SPSS) software (Version 22; SPSS Inc., Chicago, IL). The Kruskal-Wallis test was

used to examine the differences in mean percent gap volume and mean percent porosity between the 4 groups. Mann-Whitney's U test was performed to identify any significant differences between groups. Significance was set at $P < .05$.

Wilcoxon signed rank test was used to compare mean percent gap volume and mean percent porosity between levels and time points within the same group with a significance level of $P < .05$.



CHAPTER IV

RESEARCH RESULTS

Representative 3D reconstructive image of each group were shown in figure 15 to 18. These images were divided into 3 levels; external 1/3 (contact with blood or NSS), middle 1/3 and internal 1/3. Greater number of porosity and gap volume was observed only within external 1/3 (0.5 mm portion from contact surface) of the samples (figure 15 to 18 D, G). Two-dimension cuts indicated poorly adaptation to cavity wall at the external 1/3 (figure 15 to 18 D, G). Middle 1/3 and internal 1/3 of material were shown to be well adapted to dentine wall (figure 15 to 18 B, C, E, F).

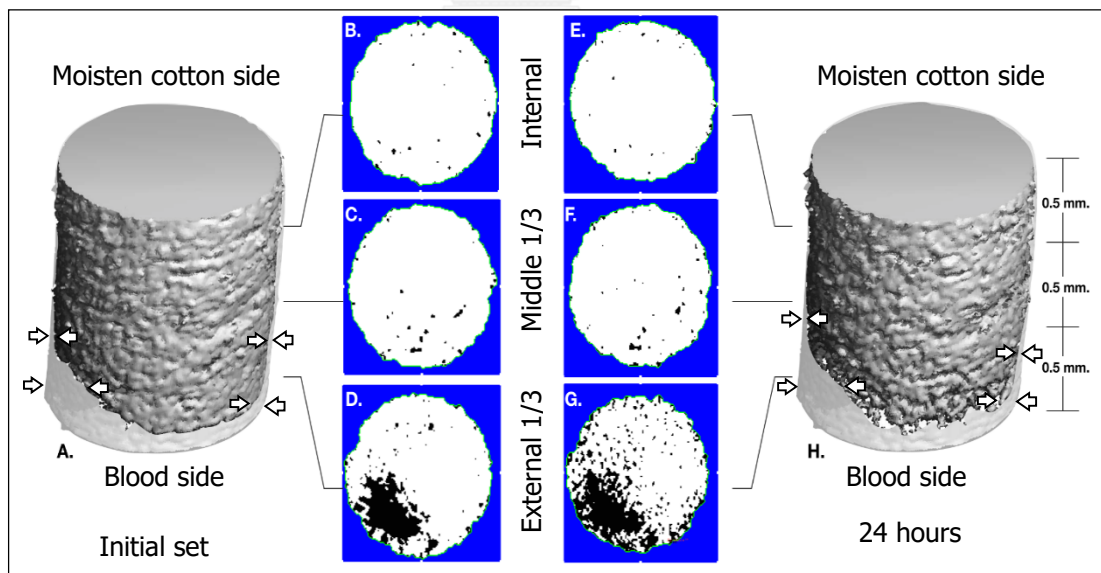


Figure 15: A Biodentine/Blood sample (A) 3D reconstruction of Biodentine and gap (arrows) at initial set; (B-D) random 2D images of internal 1/3, middle 1/3 and external 1/3, respectively. (H) 3D reconstruction of Biodentine and gap (arrows) at 24 hours; (E-G) random 2D images of internal 1/3, middle 1/3 and external 1/3, respectively. Black scatter within the material represents porosity.

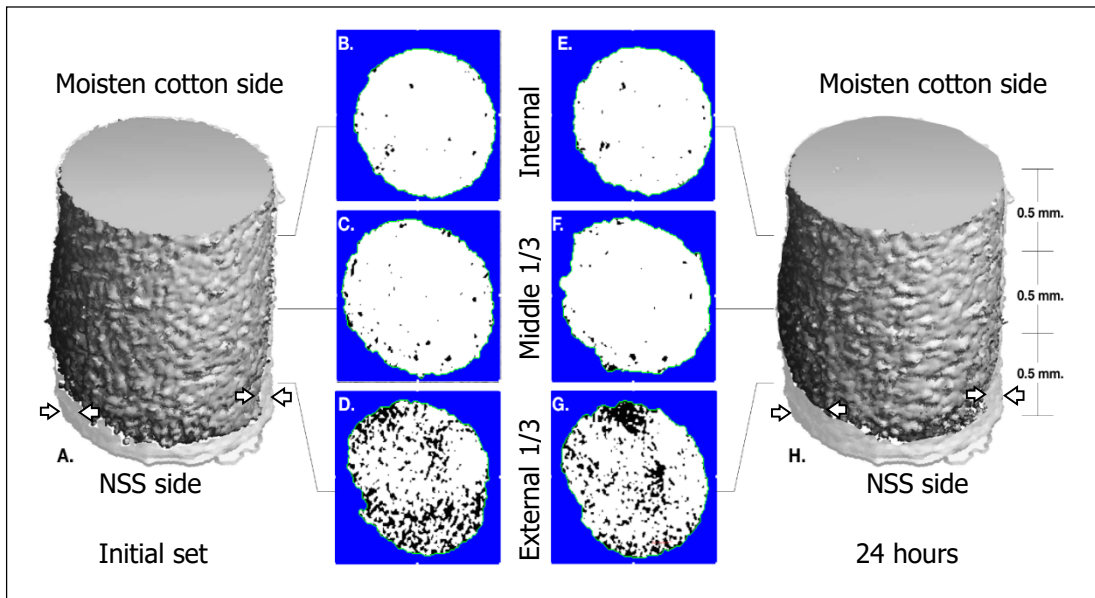


Figure 16: A Biodentine/NSS sample (A) 3D reconstruction of Biodentine and gap (arrows) at initial set; (B-D) random 2D images of internal 1/3, middle 1/3 and external 1/3, respectively. (H) 3D reconstruction of Biodentine and gap (arrows) at 24 hours; (E-G) random 2D images of internal 1/3, middle 1/3 and external 1/3, respectively. Black scatter within the material represents porosity.

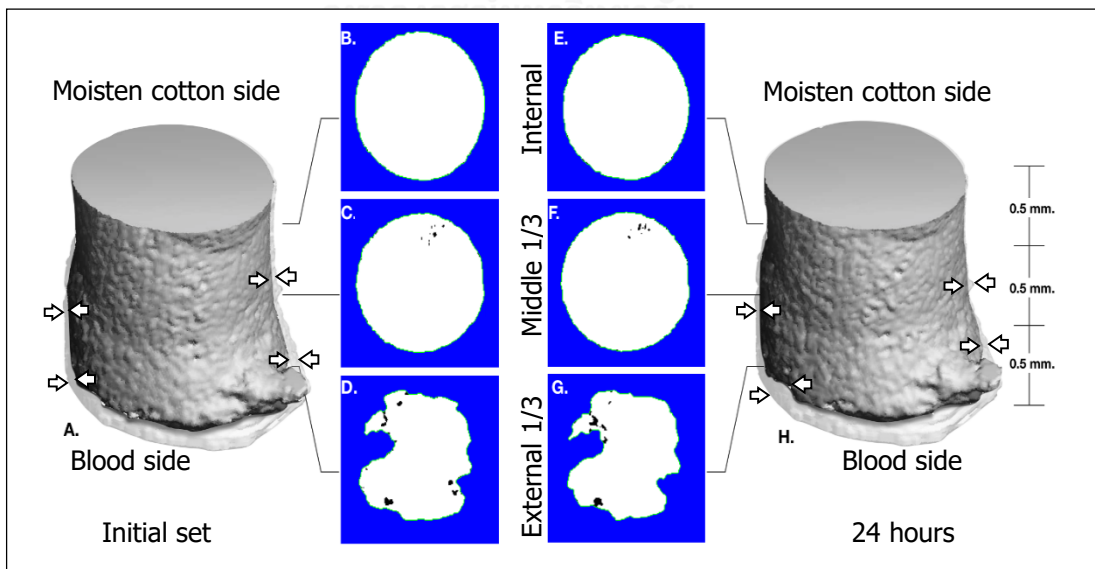


Figure 17: A MTA/Blood sample (A) 3D reconstruction of MTA and gap (arrows) at initial set; (B-D) random 2D images of internal 1/3, middle 1/3 and external 1/3, respectively.

(H) 3D reconstruction of MTA and gap (arrows) at 24 hours; (E-G) random 2D images of internal 1/3, middle 1/3 and external 1/3, respectively. Black scatter within the material represents porosity.

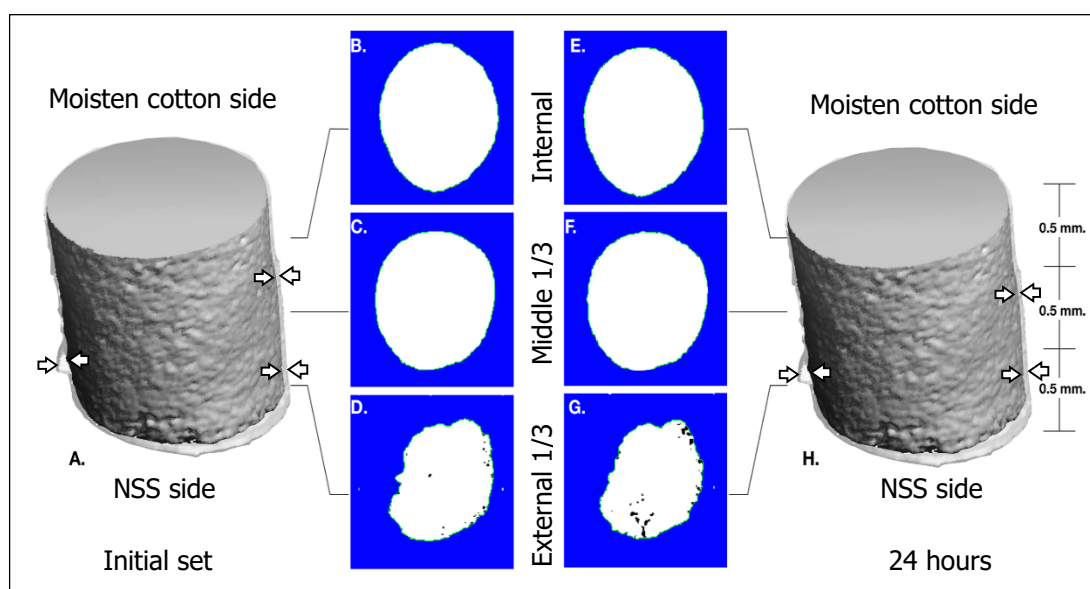


Figure 18: A MTA/NSS sample (A) 3D reconstruction of MTA and gap (arrows) at initial set; (B-D) random 2D images of internal 1/3, middle 1/3 and external 1/3, respectively. (H) 3D reconstruction of MTA and gap (arrows) at 24 hours; (E-G) random 2D images of internal 1/3, middle 1/3 and external 1/3, respectively. Black scatter within the material represents porosity.

As the data in this study were not normally distributed, non-parametric tests were indicated.

Percent gap volume

Percent gap volume was calculated from difference between cavity volume and material volume (figure 14). Percent gap volume at initial setting time and 24 hours of each group were shown in appendix A (table 5). Mean

percent gap volume at 24 hours were significantly higher than initial setting in MTA/Blood but not significantly different in other groups (Wilcoxon signed rank test, $P < .05$) (figure 19).

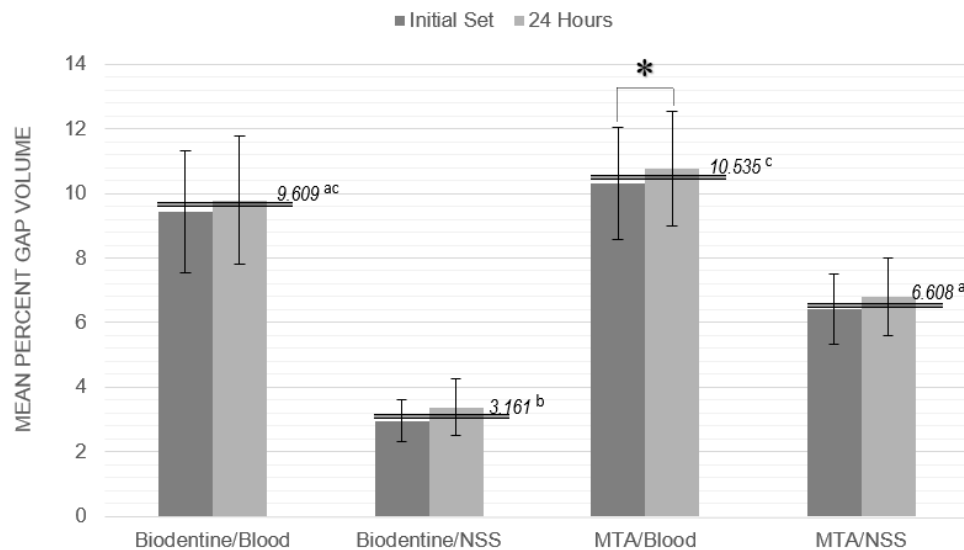


Figure 19: Mean percent gap volume at initial set and 24 hours. I-bar represents standard errors. Double line and italic numbers represent mean percent gap volume of combined data of both time points. The same superscript letters were not significantly different of combined data of both time points (Mann-Whitney's U test, $P < .05$). * indicates significant difference between time points within groups (Wilcoxon signed rank test, $P < .05$).

Mean percent gap volume of combined data of both time points of each group was shown in table 2 and appendix A (table 4). Mean percent gap volume of Biodentine/Blood was not significantly different from MTA/Blood. Blood contamination increase mean percent gap volume in both type of materials significantly (Mann-Whitney's U test, $P < .05$). Biodentine/NSS had

significantly lower mean percent gap volume compared with MTA/NSS (Mann-Whitney's U test, $P < .05$) (table 2).

Table 2: Mean percent gap volume (95% Confidence Interval for Mean) of combined data of both time points.

Contamination	Material	
	Biodentine	MTA
Blood	9.609 (6.699, 12.320) ^{ac}	10.535 (8.098, 12.972) ^c
Normal saline	3.161 (2.087, 4.236) ^b	6.608 (5.008, 8.207) ^a

The same superscript letters were not significantly different (Mann-Whitney's U test, $P < .05$).

Mean percent gap volume at initial setting time and 24 hours were shown in figure 20. At initial setting time, Biodentine/NSS had significantly lower mean percent gap volume compared with other groups ($P < .05$). There was no significant difference between Biodentine/Blood, MTA/Blood and MTA/NSS groups. At 24 hours, blood contamination increase mean percent gap volume in both type of materials significantly (Mann-Whitney's U test, $P < .05$). Mean percent gap volume of Biodentine/Blood was not significantly different from MTA/Blood. Biodentine/NSS had significantly lower mean percent gap volume compared with MTA/NSS, MTA/Blood and Biodentine/Blood (Mann-Whitney's U test, $P < .05$) (Figure 20).

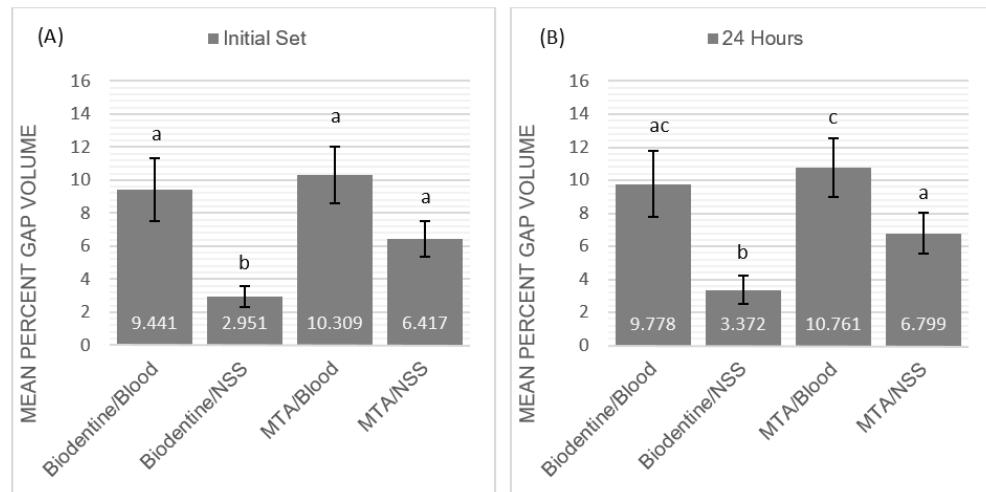


Figure 20: Mean percent gap volume at (A) initial set and (B) 24 hours. I-bar represents standard errors. The same superscript letters were not significantly different (Mann-Whitney's U test, $P < .05$).

Mean percent gap volume of external 1/3, middle 1/3 and internal 1/3 of each experimental group was shown in figure 21 and in appendix A (table 6). In all groups, the mean percent gap volume of external 1/3 were significantly higher than middle 1/3 and internal 1/3 (Wilcoxon signed rank test, $P < .05$). In Biodentine/NSS, mean percent gap volume of internal 1/3 was higher than middle 1/3 significantly (Wilcoxon signed rank test, $P < .05$). In MTA/Blood, mean percent gap volume of middle 1/3 was higher than internal 1/3 significantly (Wilcoxon signed rank test, $P < .05$) (figure 21). In Biodentine/Blood and MTA/NSS, there was no significant difference in mean percent gap volume of middle 1/3 and internal 1/3 (Wilcoxon signed rank test, $P < .05$).

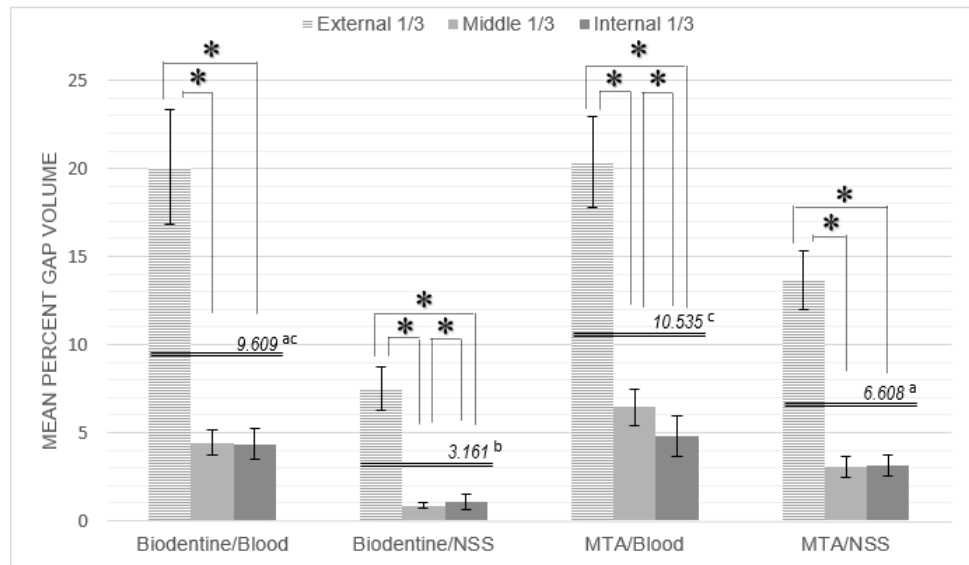


Figure 21: Mean percent gap volume at external 1/3, middle 1/3 and internal 1/3. I-bar represents standard errors. Double line and italic numbers represent mean percent gap volume of combined data of all 3 levels. The same superscript letters were not significantly different of combined data of all 3 levels (Mann-Whitney's U test, $P < .05$). * indicates significant difference between levels within group (Wilcoxon signed rank test, $P < .05$).

Percent porosity

Mean percent porosity at initial setting time and 24 hours of each groups were shown in appendix B (table 8). There was no significantly difference in mean percent porosity between time points in all groups except for Biodentine/Blood, which showed significantly higher mean percent porosity at 24 hours (Wilcoxon signed rank test, $P < .05$) (figure 22).

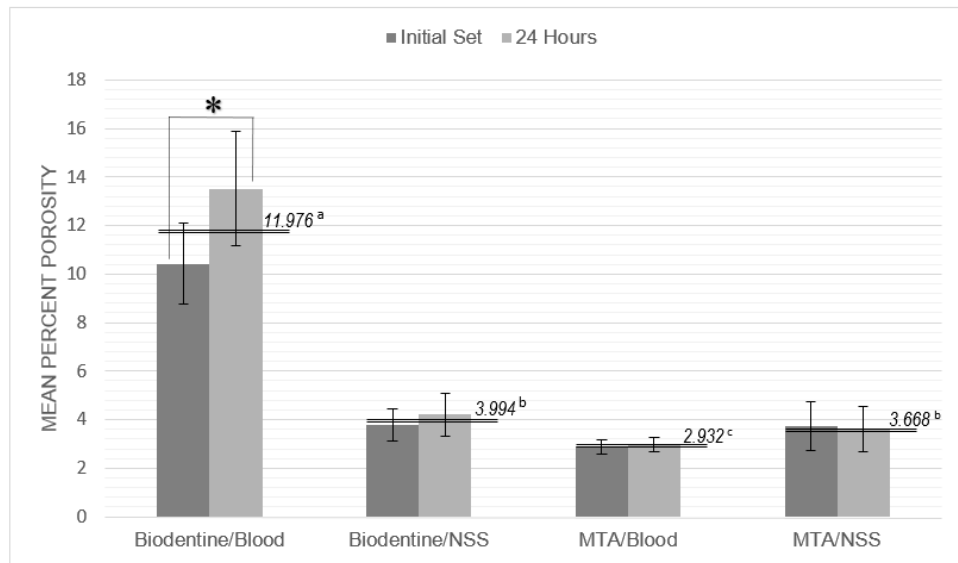


Figure 22: Mean percent porosity at initial set and 24 hours. I-bar represents standard errors. Double line and italic numbers represent mean percent porosity of combined data of both time points. The same superscript letters were not significantly different of combined data of both time points (Mann-Whitney's U test, $P < .05$). * indicates significantly difference between time points within groups (Wilcoxon signed rank test, $P < .05$).

Mean percent porosity of combined data of both time points of each group was shown in table 3 and in appendix B (table 7). Biodentine/Blood had significantly higher mean percent porosity than Biodentine/NSS, MTA/Blood and MTA/NSS (Mann-Whitney's U test, $P < .05$). MTA/Blood had significantly lower mean percent porosity than Biodentine/Blood, Biodentine/NSS and MTA/NSS (Mann-Whitney's U test, $P < .05$). There was no significant difference in mean percent porosity between Biodentine/NSS and MTA/NSS (Mann-Whitney's U test, $P < .05$) (table 3).

Table 3: Mean percent porosity (95% Confidence Interval for Mean) of combined data of both time points.

Contamination	Material	
	Biodentine	MTA
Blood	11.976 (9.128, 14.822) ^a	2.932 (2.510, 3.352) ^c
Normal saline	3.994 (2.894, 5.094) ^b	3.668 (2.308, 5.027) ^b

The same superscript letters were not significantly different (Mann-Whitney's U test, $P < .05$).

Mean percent porosity at initial setting time and 24 hours were shown in figure 23. At initial setting time, Biodentine/Blood had significantly higher mean percent porosity than MTA/Blood, Biodentine/NSS and MTA/NSS ($P < .05$). Mean percent porosity of Biodentine/NSS was not different from MTA/Blood or MTA/NSS. While Biodentine/Blood had significantly higher mean percent porosity than Biodentine/NSS, mean percent porosity of MTA/Blood was significantly lower than MTA/NSS ($P < .05$). At 24 hours, Biodentine/Blood had significantly higher mean percent porosity than MTA/Blood, Biodentine/NSS and MTA/NSS ($P < .05$). Mean percent porosity of Biodentine/NSS was not different from MTA/NSS. Mean percent porosity of MTA/Blood was significantly lower than MTA/NSS, Biodentine/NSS and Biodentine/Blood ($P < .05$). (figure 23)

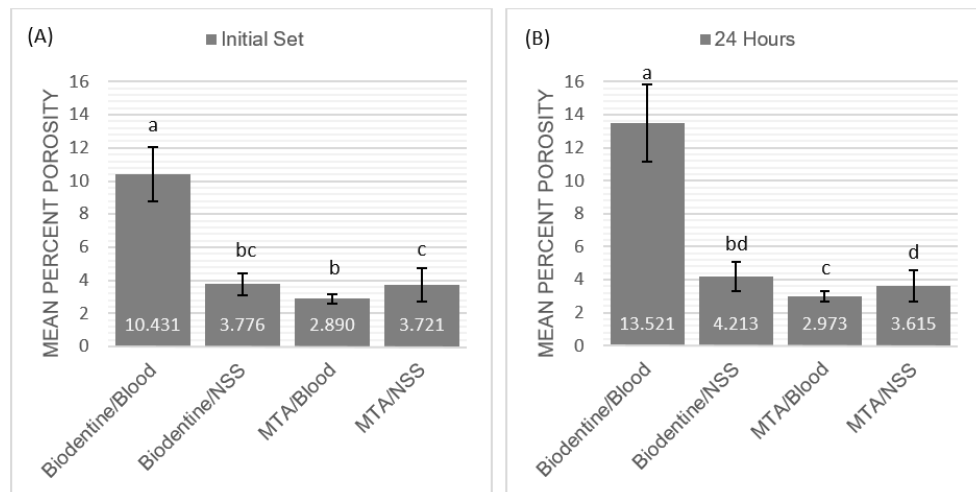


Figure 23: Mean percent porosity at (A) initial set and (B) 24 hours. I-bar represents standard errors. The same superscript letters were not significantly different (Mann-Whitney's U test, $P < .05$).

Mean percent porosity of external 1/3, middle 1/3 and internal 1/3 of each experimental group was shown in figure 24 and in appendix B (table 9). In all groups, the mean percent porosity of external 1/3 were significantly higher than middle 1/3 and internal 1/3 (Wilcoxon signed rank test, $P < .05$). The mean percent porosity of middle 1/3 of each experimental group was not significantly different from internal 1/3, except for MTA/NSS, the mean percent porosity of middle 1/3 was significantly lower than internal 1/3 (Wilcoxon signed rank test, $P < .05$).

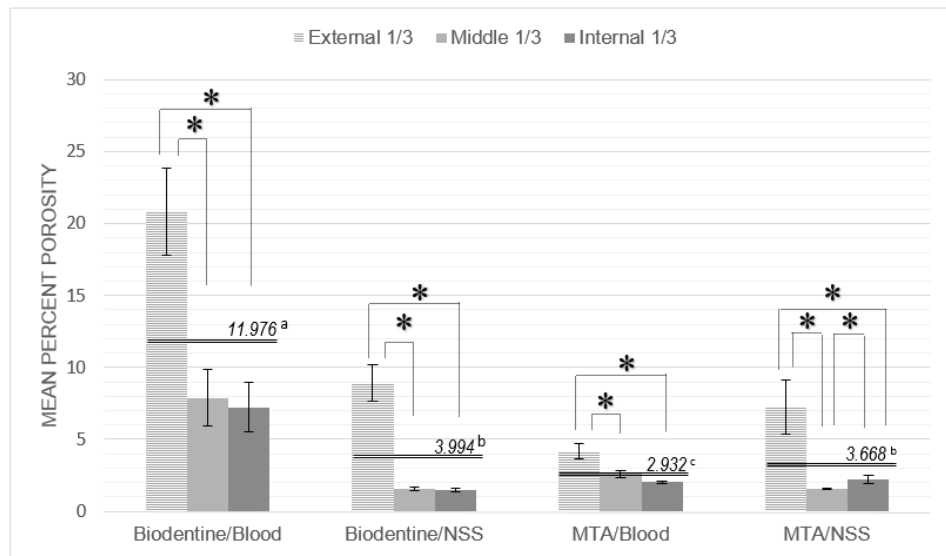


Figure 24: Mean percent porosity at external 1/3, middle 1/3 and internal 1/3. I-bar represents standard errors. Double line and italic numbers represent mean percent porosity of combined data of all 3 levels. The same superscript letters were not significantly different of combined data of all 3 levels (Mann-Whitney's U test, $P < .05$). * indicates significantly difference between levels within group (Wilcoxon signed rank test, $P < .05$).

CHAPTER V

DISCUSSION

Many studies on marginal adaptation and porosity used sectioning method such as observation under scanning electron microscope (SEM) (66, 69, 79). In our pilot study, an attempt was made to observe cross-sectional cut of repair material within cavity under SEM. However, high-vacuums evaporation led to excess cracks and widened the gap between material and dentin wall. Micro-CT method could observe material without processing the samples. Processing of material also led to loss of material (75). On the other hand, using micro-CT, observation immediately during setting was possible (71).

Literature classified porosity into 3 major types: closed, through and blind porosity (80). Closed porosity is completely surrounded by material mass. Blind porosity originates from the external surface of material on either the free surface or dentin-material interface with definite termination within material mass. Through porosity is the continuous connection between 2 opposite surfaces of material mass. Closed porosity impacts mechanical properties of material (81). Through and blind porosity influences oral fluid penetration (81). From this study, gap volume included

blind porosity at the interface, while porosity consisted of close porosity and through porosity. The result of this study could imply that blood contamination affects all types of porosity which may impact on mechanical properties and oral fluid penetration.

MTA is a Portland cement derivative. It is made from natural material, whereas Biodentine is laboratory synthesized. MTA contains impurities of naturally derived material in contrast to Biodentine which is purified. Biodentine is only composed of tricalcium silicate and dicalcium silicate in controlled proportion with particle size of 2 μm (9) which could penetrate into the dentinal tubules to form tag-like structure (82). On the other hand, components of MTA are tricalcium silicate, dicalcium silicate, tricalcium aluminate and other metal oxides which have particle size between $<1 \mu\text{m}$ to 50 μm (24). Dentinal tubule penetration was not found in MTA (83). Biodentine contains setting accelerator and the hydrosoluble polymer superplasticizer while MTA does not. Hydrosoluble polymer superplasticizer has surfactant effect which provides better flowability characteristic for Biodentine (43). Owing to smaller particle size and superplasticizer, without blood contamination, mean percent gap volume in Biodentine was lower than MTA. From Sarkar *et al.* (84), gap between MTA and dentin was completely filled with hydroxyapatite. Sarkar *et al.*'s study used the phosphate

buffered saline to simulate tissue fluid instead of normal saline. In order to create a good marginal adaptation of MTA, calcium ions from MTA had to be contacted with phosphate ions from phosphate buffered saline to produce hydroxyapatite crystals (85). With MTA surface exposed to normal saline in our study, there might be an effect from sodium chloride on MTA setting. Sodium chloride had been reported to act as a retarder (86).

In this study, initial scanning was performed at 6 minutes and 45 minutes because of manufacturers' claim as initial setting time of Biodentine (9) and MTA (38), respectively. Second scanning period was chosen at 24 hours because it represented second clinical appointment for MTA setting evaluation. Blood contamination delayed MTA setting to 36 hours (87). Therefore, in blood contamination condition in this study, the material may not be completely set at 24 hours. A short setting time of the material reduces the possibility of any reaction interferences. In our study, increasing of gap volume in MTA/Blood and porosity in Biodentine/Blood were observed after initial setting time. This might be due to altered initial setting time of both blood contaminated materials. Recent study showed that setting time of blood contaminated Biodentine was delayed to 46 minutes (88). Delayed setting time of blood contaminated Biodentine increased the possibility of effect of blood upon initial

setting. This might result in higher porosity of Biodentine/Blood observed at 24 hours. Increased water-to-powder ratio prolongs setting time of MTA (28).

Blood contamination affects hydration reaction of silicate based material such as MTA (89). Blood contains cells and proteins such as hemoglobin. In this study, equal amount of blood and normal saline was used on the experimental surface (external 1/3). Main difference between blood contaminated and NSS groups was hemoglobin and other proteins, which were present only in blood contamination groups. Cells and proteins from blood could obscure the dentinal tubules and prevent adaptation at the interface between the repair material and dentin walls (78). This might explain the significantly higher gap volume observed in both blood contaminated materials.

Surfactants are surface-active chemicals which used for air entraining and reduction of water in concrete mixture. They are classified into 2 types according to their purposes: air-entraining surfactant and plasticizing or water-reducing surfactant (37). Air-entraining surfactants, such as hemoglobin and other proteins in blood, promote bubble formation and results in porosity of the mixture (36, 37). Plasticizing or water-reducing surfactant, such as polycarboxylate hydrosoluble polymer in Biodentine, makes cement particle hydrophilic and well-dispersed in the water (37).

This dispersion could allow the exceed amount of water from blood to incorporate into setting material. Increased water-to-powder ratio causes more porosity (35) and prolong setting time (28). This resulted in higher chance of Biodentine particle to be affected by hemoglobin and other proteins. Combined plasticizing surfactant effects of superplasticizer and air-entraining surfactant effect of hemoglobin and other proteins in Biodentine/Blood might lead to significantly higher porosity. Without superplasticizer, MTA had lower chance to incorporate with blood as their particles were not dispersed. Compared with distilled water in MTA mixture, blood in CollaTape has higher osmotic pressure due to hemoglobin (90). Water from MTA mixture might migrate out into blood soaked CollaTape. With losing of water of MTA mixture adjunct to blood contamination, porosity was decreased.

Previous studies reported that blood contamination had many effects to MTA such as microstructure, mechanical properties, retention and marginal adaptation (25, 41, 78, 79, 89). SEM micrograph showed that MTA mixed with blood had more porous microstructure and lacked of acicular crystal formation of the material (89). Decreasing of compressive strength of blood contaminated MTA was related to increasing of porosity (41). Push-out test shows that blood contamination decreased retention of MTA in simulated furcation perforations (25). Leakage prevention is vital to prognosis

of perforation repair (20). While Torabinejad *et al.* showed that presence or absence of blood had no significant effect on the amount of dye leakage into 2-mm depth root end cavity (63), the SEM study by Milani *et al.* concluded that exposure to blood during setting has a negative effect on marginal adaptation of MTA (78).

In each group, sample was divided into 3 levels in order to investigate the difference between the different parts of the material. We found that the majority of effect from blood contamination was in the external 1/3. Valois *et al.* (91) suggested that minimum of thickness that could prevent leakage of MTA when use as apical barrier is 4 mm. Most of most of root thickness at the furcation are only between 1.2-2.38 mm (92). In perforation situation, this results in less than 3-mm thickness of material in most cases. From current study, we found that blood contamination had impacts on marginal adaptation and porosity only within 0.5 mm from the contact surface. As we did not mix the material with blood, effect from blood contamination on porosity was noticed mainly at the external 1/3, which approximated to the blood contamination surface.

Although Biodentine came in pre-proportional capsule and definite instruction of application, consistency of the mixture was not uniform in every capsule after

mixing. In this study, after mixing by an amalgamator, Biodentine mixing had to be continued manually. Both MTA and Biodentine involved with manual mixing and manual application. The consistency of material in each sample might not be uniformed and resulted in high standard deviation of the data in this study.

In clinical situation, contamination of repair material could impact adequate repair. Higher gap volume in blood contaminated Biodentine and MTA was observed in both materials. Blood contamination increased porosity significantly in Biodentine. From the result of this study, Biodentine could be used as a single visit perforation repair material, but appropriate homeostasis should be carried out to achieve the benefits of this novel material.

Limitations

Only furcal floor of human lower mandibular molar used in this study to lower anatomical variation of samples as it may not reflect other location on the other type of tooth.

Because of through porosity was inside the material mass, closed porosity and through porosity could not be distinguished in this study.

Although micro-CT used in this study is performed non-destructively on incomplete set material, data obtained from micro-CT scanning reflects only radiopaque part of sample. With this method radiolucent part cannot be observed.

Only porosity can be directly obtained from each scanning. Gap volume had to be calculated the difference between cavity volume and material volume. Error of gap volume measurement in this study could be effected by the errors from both cavity volume and material volume measurements.

This is a laboratory study, it may not represent clinical situation and outcomes. Further *in vivo* or clinical study will provide better understand of outcome of this novel repair material.

Conclusion

In blood contamination condition, there was no difference in marginal adaptation between Biodentine and MTA. Blood contamination significantly increased gap volume of both materials. In contrast, Biodentine had significantly higher porosity than MTA in blood contaminated condition. Biodentine could be used as a single visit perforation repair material under appropriate hemostasis.

REFERENCES

1. Rotstein IJHS. The endo-perio lesion: a critical appraisal of the disease condition. *Endodontic Topics*. 2006;13:34–56.
2. Torabinejad M, Hong CU, Pitt Ford TR, Kettering JD. Cytotoxicity of four root end filling materials. *Journal of endodontics*. 1995;21(10):489-92.
3. Torabinejad M, Parirokh M. Mineral trioxide aggregate: a comprehensive literature review--part II: leakage and biocompatibility investigations. *Journal of endodontics*. 2010;36(2):190-202.
4. Parirokh M, Torabinejad M. Mineral trioxide aggregate: a comprehensive literature review--Part I: chemical, physical, and antibacterial properties. *Journal of endodontics*. 2010;36(1):16-27.
5. Nandini S, Ballal S, Kandaswamy D. Influence of glass-ionomer cement on the interface and setting reaction of mineral trioxide aggregate when used as a furcal repair material using laser Raman spectroscopic analysis. *Journal of endodontics*. 2007;33(2):167-72.
6. Saghiri MA, Lotfi M, Saghiri AM, Vosoughhosseini S, Fatemi A, Shiezadeh V, et al. Effect of pH on sealing ability of white mineral trioxide aggregate as a root-end filling material. *Journal of endodontics*. 2008;34(10):1226-9.
7. Borkar SA, Ataide I. Biodentine pulpotomy several days after pulp exposure: Four case reports. *J Conserv Dent*. 2015;18(1):73-8.
8. Nowicka A, Lipski M, Parafiniuk M, Sporniak-Tutak K, Lichota D, Kosierkiewicz A, et al. Response of human dental pulp capped with biodentine and mineral trioxide aggregate. *Journal of endodontics*. 2013;39(6):743-7.
9. Biodentine Scientific File [press release]. Saint Maur des Fossés Cedex, France: Septodont2010.
10. Chong BS, Pitt Ford TR, Hudson MB. A prospective clinical study of Mineral Trioxide Aggregate and IRM when used as root-end filling materials in endodontic surgery. *International endodontic journal*. 2003;36(8):520-6.

11. Maltezos C, Glickman GN, Ezzo P, He J. Comparison of the sealing of Resilon, Pro Root MTA, and Super-EBA as root-end filling materials: a bacterial leakage study. *Journal of endodontics*. 2006;32(4):324-7.
12. Namazikhah MS, Nekoofar MH, Sheykhrezae MS, Salariyeh S, Hayes SJ, Bryant ST, et al. The effect of pH on surface hardness and microstructure of mineral trioxide aggregate. *International endodontic journal*. 2008;41(2):108-16.
13. Fuss Z, Trope M. Root perforations: classification and treatment choices based on prognostic factors. *Endodontics & dental traumatology*. 1996;12(6):255-64.
14. Bargholz C. Perforation repair with mineral trioxide aggregate: a modified matrix concept. *International endodontic journal*. 2005;38(1):59-69.
15. Abou-Rass M, Frank AL, Glick DH. The anticurvature filing method to prepare the curved root canal. *Journal of the American Dental Association*. 1980;101(5):792-4.
16. LK B. *Endodontics*: BC Decker Inc; 2002.
17. de Chevigny C, Dao TT, Basrani BR, Marquis V, Farzaneh M, Abitbol S, et al. Treatment outcome in endodontics: the Toronto study--phase 4: initial treatment. *Journal of endodontics*. 2008;34(3):258-63.
18. de Chevigny C, Dao TT, Basrani BR, Marquis V, Farzaneh M, Abitbol S, et al. Treatment outcome in endodontics: the Toronto study--phases 3 and 4: orthograde retreatment. *Journal of endodontics*. 2008;34(2):131-7.
19. Alhadainy HA, Himel VT. An in vitro evaluation of plaster of Paris barriers used under amalgam and glass ionomer to repair furcation perforations. *Journal of endodontics*. 1994;20(9):449-52.
20. Imura N, Pinheiro ET, Gomes BP, Zaia AA, Ferraz CC, Souza-Filho FJ. The outcome of endodontic treatment: a retrospective study of 2000 cases performed by a specialist. *Journal of endodontics*. 2007;33(11):1278-82.
21. Ford TR, Torabinejad M, McKendry DJ, Hong CU, Kariyawasam SP. Use of mineral trioxide aggregate for repair of furcal perforations. *Oral surgery, oral medicine, oral pathology, oral radiology, and endodontics*. 1995;79(6):756-63.

22. Lee SJ, Monsef M, Torabinejad M. Sealing ability of a mineral trioxide aggregate for repair of lateral root perforations. *Journal of endodontics*. 1993;19(11):541-4.
23. Holland R, De Souza V, Nery MJ, Otoboni Filho JA, Bernabé PFE, Dezan E. Reaction of dogs' teeth to root canal filling with mineral trioxide aggregate or a glass ionomer sealer. *Journal of endodontics*. 1999;25(11):728-30.
24. Camilleri J. Hydration mechanisms of mineral trioxide aggregate. *International endodontic journal*. 2007;40(6):462-70.
25. Vanderweele RA, Schwartz SA, Beeson TJ. Effect of blood contamination on retention characteristics of MTA when mixed with different liquids. *Journal of endodontics*. 2006;32(5):421-4.
26. Asgary S, Parirokh M, Eghbal MJ, Brink F. Chemical differences between white and gray mineral trioxide aggregate. *Journal of endodontics*. 2005;31(2):101-3.
27. Hwang YC, Lee SH, Hwang IN, Kang IC, Kim MS, Kim SH, et al. Chemical composition, radiopacity, and biocompatibility of Portland cement with bismuth oxide. *Oral surgery, oral medicine, oral pathology, oral radiology, and endodontics*. 2009;107(3):e96-102.
28. Cavenago BC, Pereira TC, Duarte MA, Ordinola-Zapata R, Marciano MA, Bramante CM, et al. Influence of powder-to-water ratio on radiopacity, setting time, pH, calcium ion release and a micro-CT volumetric solubility of white mineral trioxide aggregate. *International endodontic journal*. 2013.
29. Chogle S, Mickel AK, Chan DM, Huffaker K, Jones JJ. Intracanal assessment of mineral trioxide aggregate setting and sealing properties. *General dentistry*. 2007;55(4):306-11.
30. Nekoofar MH, Adusei G, Sheykhrezae MS, Hayes SJ, Bryant ST, Dummer PM. The effect of condensation pressure on selected physical properties of mineral trioxide aggregate. *International endodontic journal*. 2007;40(6):453-61.

31. Islam I, Chng HK, Yap AU. Comparison of the physical and mechanical properties of MTA and portland cement. *Journal of endodontics*. 2006;32(3):193-7.
32. Dammaschke T, Gerth HU, Zuchner H, Schafer E. Chemical and physical surface and bulk material characterization of white ProRoot MTA and two Portland cements. *Dental materials : official publication of the Academy of Dental Materials*. 2005;21(8):731-8.
33. Torabinejad M, Hong CU, McDonald F, Pitt Ford TR. Physical and chemical properties of a new root-end filling material. *Journal of endodontics*. 1995;21(7):349-53.
34. Fridland M, Rosado R. MTA solubility: a long term study. *Journal of endodontics*. 2005;31(5):376-9.
35. Fridland M, Rosado R. Mineral trioxide aggregate (MTA) solubility and porosity with different water-to-powder ratios. *Journal of endodontics*. 2003;29(12):814-7.
36. Jasiczak J, Zielinski K. Effect of protein additive on properties of mortar. *Cement and Concrete Composites*. 2006;28(5):451-7.
37. P. Mehta PJMM. *Concrete microstructure, properties, and materials*. 3rd ed. New York: McGraw-Hill Education Companies; 2006. p. 284-6.
38. Chng HK, Islam I, Yap AU, Tong YW, Koh ET. Properties of a new root-end filling material. *J Endod*. 2005;31(9):665-8.
39. Torabinejad M, Smith PW, Kettering JD, Pitt Ford TR. Comparative investigation of marginal adaptation of mineral trioxide aggregate and other commonly used root-end filling materials. *Journal of endodontics*. 1995;21(6):295-9.
40. Boutsoukis C, Noula G, Lambrianidis T. Ex vivo study of the efficiency of two techniques for the removal of mineral trioxide aggregate used as a root canal filling material. *Journal of endodontics*. 2008;34(10):1239-42.
41. Nekoofar MH, Stone DF, Dummer PM. The effect of blood contamination on the compressive strength and surface microstructure of mineral trioxide aggregate. *International endodontic journal*. 2010;43(9):782-91.

42. E.M. Gartner JFY DAD, I. Jawed. Hydration of portland cement. In: PB JB, editor. *The Structure and Performance of Cements*. 2 ed. London: Spon Press; 2002.
43. Wongkornchaowalit N, Lertchirakarn V. Setting time and flowability of accelerated Portland cement mixed with polycarboxylate superplasticizer. *Journal of endodontics*. 2011;37(3):387-9.
44. Wang X, Sun H, Chang J. Characterization of Ca₃SiO₅/CaCl₂ composite cement for dental application. *Dental materials : official publication of the Academy of Dental Materials*. 2008;24(1):74-82.
45. Darvell BW, Wu RC. "MTA"-an Hydraulic Silicate Cement: review update and setting reaction. *Dental materials : official publication of the Academy of Dental Materials*. 2011;27(5):407-22.
46. Camilleri J, Montesin FE, Curtis RV, Ford TR. Characterization of Portland cement for use as a dental restorative material. *Dental materials : official publication of the Academy of Dental Materials*. 2006;22(6):569-75.
47. Zingg A, Winnefeld F, Holzer L, Pakusch J, Becker S, Figi R, et al. Interaction of polycarboxylate-based superplasticizers with cements containing different C 3 A amounts. *Cement and Concrete Composites*. 2009;31(3):153-62.
48. Camilleri J. The physical properties of accelerated Portland cement for endodontic use. *International endodontic journal*. 2008;41(2):151-7.
49. Camilleri J, Sorrentino F, Damidot D. Investigation of the hydration and bioactivity of radiopacified tricalcium silicate cement, Biodentine and MTA Angelus. *Dental materials : official publication of the Academy of Dental Materials*. 2013;29(5):580-93.
50. Camilleri J, Montesin FE, Brady K, Sweeney R, Curtis RV, Ford TRP. The constitution of mineral trioxide aggregate. *Dental Materials*. 2005;21(4):297-303.
51. Guneser MB, Akbulut MB, Eldeniz AU. Effect of various endodontic irrigants on the push-out bond strength of biodentine and conventional root perforation repair materials. *Journal of endodontics*. 2013;39(3):380-4.

52. Keiser K, Johnson CC, Tipton DA. Cytotoxicity of mineral trioxide aggregate using human periodontal ligament fibroblasts. *Journal of endodontics*. 2000;26(5):288-91.
53. Torabinejad M, Hong CU, Lee SJ, Monsef M, Pitt Ford TR. Investigation of mineral trioxide aggregate for root-end filling in dogs. *Journal of endodontics*. 1995;21(12):603-8.
54. Kettering JD, Torabinejad M. Investigation of mutagenicity of mineral trioxide aggregate and other commonly used root-end filling materials. *Journal of endodontics*. 1995;21(11):537-9.
55. Asrari M, Lobner D. In vitro neurotoxic evaluation of root-end-filling materials. *Journal of endodontics*. 2003;29(11):743-6.
56. Masuda Y, Wang X, Hossain M, Unno A, Jayawardena J, Saito K, et al. Evaluation of biocompatibility of mineral trioxide aggregate with an improved rabbit ear chamber. *Journal of oral rehabilitation*. 2005;32(2):145-50.
57. Tunca YM, Aydin C, Ozen T, Seyrek M, Ulusoy HB, Yildiz O. The effect of mineral trioxide aggregate on the contractility of the rat thoracic aorta. *Journal of endodontics*. 2007;33(7):823-6.
58. Zhou H-m, Shen Y, Wang Z-j, Li L, Zheng Y-f, Häkkinen L, et al. In vitro cytotoxicity evaluation of a novel root repair material. *Journal of endodontics*. 2013;39(4):478-83.
59. Laurent P, Camps J, About I. Biodentine(TM) induces TGF-beta1 release from human pulp cells and early dental pulp mineralization. *International endodontic journal*. 2012;45(5):439-48.
60. Nowicka A, Wilk G, Lipski M, Kołdecki J, Buczkowska-Radlińska J. Tomographic Evaluation of Reparative Dentin Formation after Direct Pulp Capping with Ca (OH) 2, MTA, Biodentine, and Dentin Bonding System in Human Teeth. *Journal of endodontics*. 2015.
61. Kayahan M, Nekoofar MH, Kazandağ M, Canpolat C, Malkondu O, Kaptan F, et al. Effect of acid-etching procedure on selected physical properties of

- mineral trioxide aggregate. *International endodontic journal*. 2009;42(11):1004-14.
62. Remadnia A, Dheilily R, Laidoudi B, Quéneudec M. Use of animal proteins as foaming agent in cementitious concrete composites manufactured with recycled PET aggregates. *Construction and Building Materials*. 2009;23(10):3118-23.
 63. Torabinejad M, Higa RK, McKendry DJ, Pitt Ford TR. Dye leakage of four root end filling materials: effects of blood contamination. *Journal of endodontics*. 1994;20(4):159-63.
 64. Stabholz A, Friedman S, Abed J. Marginal adaptation of retrograde fillings and its correlation with sealability. *Journal of endodontics*. 1985;11(5):218-23.
 65. Peters CI, Peters OA. Occlusal loading of EBA and MTA root-end fillings in a computer-controlled masticator: a scanning electron microscopic study. *International endodontic journal*. 2002;35(1):22-9.
 66. Gondim E, Zaia AA, Gomes BP, Ferraz CC, Teixeira FB, Souza-Filho FJ. Investigation of the marginal adaptation of root-end filling materials in root-end cavities prepared with ultrasonic tips. *International endodontic journal*. 2003;36(7):491-9.
 67. Shani J, Friedman S, Stabholz A, Abed J. A radionuclide model for evaluating sealability of retrograde filling materials. *International journal of nuclear medicine and biology*. 1984;11(1):46-52.
 68. Torabinejad M, Rastegar AF, Kettering JD, Ford TRP. Bacterial leakage of mineral trioxide aggregate as a root-end filling material. *Journal of endodontics*. 1995;21(3):109-12.
 69. Torabinejad M, Lee S-J, Hong C-U. Apical marginal adaptation of orthograde and retrograde root end fillings: a dye leakage and scanning electron microscopic study. *Journal of endodontics*. 1994;20(8):402-7.
 70. Sanghavi T, Shah N, Shah RR. Comparative analysis of sealing ability of biodentin and calcium phosphate cement against mineral trioxide aggregate (Mta) as a furcal perforation repair material (an in vitro study). 2013.

71. Swain MV, Xue J. State of the art of Micro-CT applications in dental research. *International journal of oral science*. 2009;1(4):177-88.
72. Chen X, Cuijpers VM, Fan MW, Frencken JE. Validation of micro-CT against the section method regarding the assessment of marginal leakage of sealants. *Australian dental journal*. 2012;57(2):196-9.
73. Peters O, Laib A, Rügsegger P, Barbakow F. Three-dimensional analysis of root canal geometry by high-resolution computed tomography. *Journal of Dental Research*. 2000;79(6):1405-9.
74. Ho ST, Hutmacher DW. A comparison of micro CT with other techniques used in the characterization of scaffolds. *Biomaterials*. 2006;27(8):1362-76.
75. Sun J, Lin-Gibson S. X-ray microcomputed tomography for measuring polymerization shrinkage of polymeric dental composites. *Dental materials*. 2008;24(2):228-34.
76. Sun J, Eidelman N, Lin-Gibson S. 3D mapping of polymerization shrinkage using X-ray micro-computed tomography to predict microleakage. *dental materials*. 2009;25(3):314-20.
77. Al-Fouzan K, Al-Garawi Z, Al-Hezaimi K, Javed F, Al-Shalan T, Rotstein I. Effect of acid etching on marginal adaptation of mineral trioxide aggregate to apical dentin: microcomputed tomography and scanning electron microscopy analysis. *International journal of oral science*. 2012;4(4):202-7.
78. Rahimi S, Ghasemi N, Shahi S, Lotfi M, Froughreyhani M, Milani AS, et al. Effect of blood contamination on the retention characteristics of two endodontic biomaterials in simulated furcation perforations. *Journal of endodontics*. 2013;39(5):697-700.
79. Milani AS, Rahimi S, Froughreyhani M, Pakdel MV. Effect of blood contamination on marginal adaptation and surface microstructure of mineral trioxide aggregate: a SEM study. *Journal of dental research, dental clinics, dental prospects*. 2013;7(3):157.
80. Paul Webb CO. *Analytical Methods in Fine Particle Technology*: Norcross: Micrometrics Instrument Corporation; 1997.

81. Milutinovic-Nikolic AD, Medic VB, Vukovic ZM. Porosity of different dental luting cements. *Dental materials : official publication of the Academy of Dental Materials*. 2007;23(6):674-8.
82. Atmeh A, Chong E, Richard G, Festy F, Watson T. Dentin-cement Interfacial Interaction Calcium Silicates and Polyalkenoates. *Journal of dental research*. 2012;91(5):454-9.
83. Bird DC, Komabayashi T, Guo L, Opperman LA, Spears R. In vitro evaluation of dentinal tubule penetration and biomineralization ability of a new root-end filling material. *Journal of endodontics*. 2012;38(8):1093-6.
84. Sarkar N, Caicedo R, Ritwik P, Moiseyeva R, Kawashima I. Physicochemical basis of the biologic properties of mineral trioxide aggregate. *Journal of endodontics*. 2005;31(2):97-100.
85. Parirokh M, Asgary S, Eghbal MJ, Ghoddsi J, Brink F, Askarifar S, et al. The long-term effect of saline and phosphate buffer solution on MTA: an SEM and EPMA Investigation. *Iranian endodontic journal*. 2007;2(3):81.
86. Rodger S, Double D. The chemistry of hydration of high alumina cement in the presence of accelerating and retarding admixtures. *Cement and Concrete Research*. 1984;14(1):73-82.
87. Charland T, Hartwell GR, Hirschberg C, Patel R. An evaluation of setting time of mineral trioxide aggregate and EndoSequence root repair material in the presence of human blood and minimal essential media. *Journal of endodontics*. 2013;39(8):1071-2.
88. Alhodiry W, Lyons M, Chadwick R. Effect of saliva and blood contamination on the bi-axial flexural strength and setting time of two calcium-silicate based cements: Portland cement and biodentine. *Eur J Prosthodont Restor Dent*. 2014;22(1):20.
89. Nekoofar MH, Davies TE, Stone D, Basturk FB, Dummer PM. Microstructure and chemical analysis of blood-contaminated mineral trioxide aggregate. *International endodontic journal*. 2011;44(11):1011-8.

90. Van Slyke DD, Wu H, McLean FC. Studies of gas and electrolyte equilibria in the blood V. Factors controlling the electrolyte and water distribution in the blood. *Journal of Biological Chemistry*. 1923;56(3):765-849.
91. Valois CR, Costa ED. Influence of the thickness of mineral trioxide aggregate on sealing ability of root-end fillings in vitro. *Oral Surgery, Oral Medicine, Oral Pathology, Oral Radiology, and Endodontology*. 2004;97(1):108-11.
92. Tabrizizadeh M, Reuben J, Khalesi M, Mousavinasab M, Ezabadi MG. Evaluation of radicular dentin thickness of danger zone in mandibular first molars. *Journal of dentistry*. 2010;7(4):196-9.



APPENDIX A

Gap volume

Table 4: Mean percent gap volume.

Group	Mean percent gap volume	Std. Deviation	Std. Error	95% Confidence Interval for Mean		Minimum	Maximum
				Lower Bound	Upper Bound		
Biodentine/Blood	9.609	13.378	1.365	6.899	12.320	0.001	77.030
Biodentine/NSS	3.161	5.303	0.541	2.087	4.236	0.001	29.935
MTA/Blood	10.535	12.026	1.227	8.098	12.972	0.001	66.882
MTA/NSS	6.608	7.894	0.806	5.008	8.207	0.001	32.477

Table 5: Mean percent gap volume at initial set and 24 hours.

Group	Time point	Mean percent gap volume	Std. Deviation	Std. Error	95% Confidence Interval for Mean		Minimum	Maximum
					Lower Bound	Upper Bound		
Biodentine/Blood	Initial set	9.441	13.142	1.897	5.625	13.257	0.001	75.262
	24 Hours	9.778	13.748	1.984	5.786	13.770	0.001	77.030
Biodentine/NSS	Initial set	2.951	4.506	0.650	1.642	4.259	0.001	21.927
	24 Hours	3.372	6.036	0.871	1.619	5.125	0.001	29.935
MTA/Blood	Initial set	10.310	11.921	1.721	6.848	13.771	0.001	65.697
	24 Hours	10.761	12.252	1.768	7.203	14.318	0.001	66.882
MTA/NSS	Initial set	6.417	7.464	1.077	4.250	8.584	0.001	26.959
	24 Hours	6.799	8.377	1.209	4.366	9.231	0.001	32.477

Table 6: Mean percent gap volume at external 1/3, middle 1/3 and internal 1/3.

Group	Levels	Mean percent gap volume	Std. Deviation	Std. Error	95% Confidence Interval for Mean		Minimum	Maximum
					Lower Bound	Upper Bound		
Biodentine/Blood	External1/3	20.081	18.394	3.252	13.450	26.713	5.853	77.030
	Middle1/3	4.420	3.992	0.706	2.981	5.860	0.001	16.996
	Internal1/3	4.326	4.939	0.873	2.545	6.107	0.001	18.178
Biodentine/NSS	External1/3	7.517	7.040	1.244	4.979	10.056	0.012	29.935
	Middle1/3	0.867	0.997	0.176	0.508	1.227	0.001	3.382
	Internal1/3	1.099	2.492	0.440	0.201	1.997	0.001	10.850
MTA/Blood	External1/3	20.364	14.691	2.597	15.068	25.661	4.444	66.882
	Middle1/3	6.451	5.883	1.040	4.330	8.572	0.874	22.833
	Internal1/3	4.790	6.460	1.142	2.461	7.119	0.001	21.977
MTA/NSS	External1/3	13.665	9.463	1.673	10.254	17.077	0.001	32.477
	Middle1/3	3.034	3.451	0.610	1.790	4.279	0.001	13.661
	Internal1/3	3.124	3.519	0.622	1.855	4.392	0.001	10.905



APPENDIX B

Porosity

Table 7: Mean percent porosity.

Group	Mean percent porosity	Std. Deviation	Std. Error	95% Confidence Interval for Mean		Minimum	Maximum
				Lower Bound	Upper Bound		
Biodentine/Blood	11.976	14.051	1.434	9.129	14.823	0.245	60.992
Biodentine/NSS	3.994	5.431	0.554	2.894	5.095	0.410	25.179
MTA/Blood	2.932	2.078	0.212	2.511	3.353	1.245	13.832
MTA/NSS	3.668	6.710	0.685	2.309	5.028	0.661	42.190

Table 8: Mean percent porosity at initial set and 24 hours.

Group	Time point	Mean percent porosity	Std. Deviation	Std. Error	95% Confidence Interval for Mean		Minimum	Maximum
					Lower Bound	Upper Bound		
Biodentine/Blood	Initial set	10.431	11.430	1.650	7.112	13.750	0.553	43.307
	24 Hours	13.520	16.233	2.343	8.807	18.234	0.245	60.992
Biodentine/NSS	Initial set	3.776	4.642	0.670	2.428	5.124	0.410	19.002
	24 Hours	4.212	6.162	0.889	2.423	6.002	0.442	25.179
MTA/Blood	Initial set	2.890	1.981	0.286	2.315	3.466	1.245	11.282
	24 Hours	2.973	2.192	0.316	2.336	3.609	1.352	13.832
MTA/NSS	Initial set	3.721	6.967	1.006	1.698	5.744	0.661	42.190
	24 Hours	3.615	6.515	0.940	1.723	5.507	1.075	40.058

Table 9: Mean percent porosity at external 1/3, middle 1/3 and internal 1/3.

Group	Levels	Mean percent porosity	Std. Deviation	Std. Error	95% Confidence Interval for Mean		Minimum	Maximum
					Lower Bound	Upper Bound		
Biodentine/Blood	External1/3	20.807	17.232	3.046	14.594	27.019	0.245	60.992
	Middle1/3	7.896	9.580	1.694	4.442	11.350	1.007	47.733
	Internal1/3	7.225	9.762	1.726	3.705	10.744	0.625	33.620
Biodentine/NSS	External1/3	8.950	7.151	1.264	6.371	11.528	0.660	25.179
	Middle1/3	1.573	0.755	0.134	1.301	1.846	0.533	3.407
	Internal1/3	1.460	0.807	0.143	1.169	1.751	0.410	4.025
MTA/Blood	External1/3	4.181	2.814	0.498	3.167	5.196	1.836	13.832
	Middle1/3	2.586	1.553	0.275	2.026	3.146	1.245	7.529
	Internal1/3	2.027	0.567	0.100	1.823	2.231	1.245	3.238
MTA/NSS	External1/3	7.233	10.755	1.901	3.355	11.110	0.661	42.190
	Middle1/3	1.577	0.185	0.033	1.510	1.643	1.163	1.830
	Internal1/3	2.195	1.550	0.274	1.637	2.754	1.274	7.297



VITA

Mr. Rangsit Makarukpinyo was born on 4th May 1985. He got bachelor degree of Doctor of Dental Surgery from Faculty of Dentistry, Srinakharinwirot University in 2009. From 2010 to present, he served the government as a lecturer at the Department of General Dentistry, Faculty of Dentistry, Srinakharinwirot University.

